

**SHORT-WAVELENGTH TECHNOLOGY AND THE POTENTIAL FOR  
DISTRIBUTED NETWORKS OF SMALL RADAR SYSTEMS**

Initial Submission: 2 October 2008

First Revision: 12 February 2009

Second Revision: 20 April 2009

David McLaughlin<sup>a</sup>, David Pepyne<sup>a</sup>, V. Chandrasekar<sup>b</sup>, Brenda Philips<sup>a</sup>, James Kurose<sup>a</sup>, Michael Zink<sup>a</sup>, Kelvin Droegemeier<sup>c</sup>, Sandra Cruz-Pol<sup>d</sup>, Francesc Junyent<sup>b</sup>, Jerald Brotzge<sup>c</sup>, David Westbrook<sup>a</sup>, Nitin Bharadwaj<sup>b</sup>, Yanting Wang<sup>b</sup>, Eric Lyons<sup>a</sup>, Kurt Hondl<sup>e</sup>, Yuxiang Liu<sup>b</sup>, Eric Knapp<sup>a</sup>, Ming Xue<sup>c</sup>, Anthony Hopf<sup>a</sup>, Kevin Kloesel<sup>c</sup>, Alfred DeFonzo<sup>a</sup>, Pavlos Kollias<sup>f</sup>, Keith Brewster<sup>c</sup>, Robert Contreras<sup>a</sup>, Theodore Djaferis<sup>a</sup>, Edin Insanic<sup>a</sup>, Stephen Frasier<sup>a</sup>, Frederick Carr<sup>c</sup>

a. University of Massachusetts, Amherst, MA 01003

b. Colorado State University, Fort Collins, CO 80523

c. University of Oklahoma, Norman, OK 73019

d. University of Puerto Rico, Mayagüez, P.R. 00681

e. National Severe Storms Laboratory, Norman, OK 73072

f. McGill University, Montreal, Quebec, Canada, H3A 2K6

---

*\* Corresponding author.* David Pepyne, Univ. of Massachusetts, 151 Holdsworth Way, Amherst, MA 01003. E-mail: pepyne@ecs.umass.edu.

## **Capsule Summary**

A new weather radar concept based on dense networks of small radars defeats the earth curvature blockage that limits today's large radars while simultaneously meeting the disparate data needs multiple end-users.

## **Abstract**

Dense networks of short-range radars capable of mapping storms and detecting atmospheric hazards are described. Comprised of small X-band (9.4-GHz) radars spaced tens of km apart, these networks defeat the earth curvature blockage that limits today's long-range weather radars and enable observing capabilities fundamentally beyond the operational state-of-the-art. These capabilities include multiple Doppler observations for mapping horizontal wind vectors, sub-km spatial resolution, and rapid-update (tens of seconds) observations extending from the boundary layer up to the tops of storms. The small physical size and low power design of these radars permits the consideration of commercial electronic manufacturing approaches and radar installation on rooftops, communications towers, and other infrastructure elements, leading to cost-effective network deployments. The networks can be architected in such a way that the sampling strategy dynamically responds to changing weather in order to simultaneously accommodate the data needs of multiple types of end-user. Such networks have the potential to supplement, or replace, the physically-large long-range civil infrastructure radars in use today.

## **1. Introduction**

Long-range microwave radar networks are an important part of the weather forecasting and warning infrastructure used by many nations today. The observing capabilities of these networks have improved considerably over the past 60 years as new technologies such as coherent high-power transmitters, solid state electronics, Doppler and dual-polarization signal processing, open software architectures and improved data dissemination and display technologies have been developed and incorporated into the system design. Taking the United States' weather radar network as an example, it is generally agreed that the improved performance and coverage of the WSR-88D (NEXRAD) system, relative to the predecessor WSR-57 and WSR-74 systems, has led to significant improvement in the short-range forecasting and warning of severe thunderstorms, tornadoes, and flash floods (Serafin and Wilson, 2000; NRC, 1995). Despite significant capability and continual improvement, one fundamental limitation of today's weather radar networks – all of which are comprised of widely-spaced radars – is the inability to observe the lower part of the atmosphere owing to the Earth's curvature and terrain blockage. Continuing with the U.S. example, the radars comprising the NEXRAD system are spaced ~230 km apart in the eastern U.S. and ~345 km in the western part of the country. This spacing prevents the system from observing more than 70% of the troposphere below 1 km altitude above ground level. A 1995 National Research Council study (NRC, 1995) investigated the adequacy of this network relative to the detection and warning of a variety of weather phenomena, including landfalling hurricanes, supercells, mesocyclones, tornado vortices, microbursts, and various types of precipitation, including snowfall. This study found that the WSR-88D network provides superior forecasting and warning capability

compared with the predecessor WSR-57 and WSR-74 systems. Nevertheless, incomplete low-level coverage and limited spatial resolution at long distance impedes the ability of this system to identify and detect small tornadoes and other fine-scale weather features. Current detection algorithms based on data from this system produce false alarm rates that are higher than desirable (NRC 2002, page 19); for example, the probability of false alarms for tornado warnings today is ~ 75% (with probability of detection ~ 72% and 14 minute lead time; data for the period 1 Oct. 2007 – 30 Sept. 2008). Westrick et al. (1999) assesses the impact of limited low-level WSR-88D coverage for detection and quantitative precipitation estimation over the U.S. west coast region. This study concluded that, as a result of significant terrain blockage in that region combined with the shallow depth of precipitation during cold seasons and low melting levels, 67-75% percent of the land surface in the region has inadequate radar coverage to support quantitative precipitation estimation.

The radars in the WSR-88D network, like those in other operational civil infrastructure radar networks deployed around the world, are physically large, high-power systems. Designed for long-range (hundreds of km) coverage through heavy precipitation, these radars must operate at radar wavelengths not subject to substantial attenuation.<sup>1</sup> This necessitates the use of large antennas to achieve the narrow beamwidth needed for km-scale spatial resolution throughout the coverage region.<sup>2</sup> The radars use high-power transmitters to meet minimum sensitivity requirements and large mechanically-scanned antennas that require dedicated land, towers, and other support infrastructure. The acquisition cost for each site, including radar equipment, land, and other installation costs, is approximately \$10M per radar, and the annual per-radar operating

---

<sup>1</sup> 10 cm (S-band) and 5 cm (C-band) are the low-attenuating wavelengths used for long-range radars.

<sup>2</sup> Achievable cross-range spatial resolution (azimuth and elevation) dictated by the antenna beamwidth, which for the WSR-88D NEXRAD radars is just under 1 deg. A 1 deg beamwidth gives a cross-range resolution of 2.8 km at 160 km range. The planned NEXRAD “super-resolution” upgrade will use signal-processing techniques to reduce the effective beamwidth (Torres and Curtis, 2006), improving the azimuth resolution to 1.4 km at 160 km.

and maintenance cost has been estimated to be \$500k (NRC 2008, page 12). The large physical size of these systems combined with potential environmental impacts limits the availability of potential sites. Moreover, scanning of the WSR-88D antenna below 0.5 degrees elevation is prohibited owing to public concerns about radiation safety. Leone et al. (1989) describe the site selection procedure for the WSR-88D radar installations. The system is jointly owned by the National Weather Service (NWS), Department of Defense (DoD), and Federal Aviation Administration (FAA), and each of these agencies established criteria for siting the radars based on factors including population distribution, climatology, approach and travel directions of severe weather, locations of airports and airways, and the location of NWS forecast offices and high-priority military and civilian facilities. The strategy for deploying national radar networks such as this is to judiciously attempt to site radars where low-altitude coverage is most needed, while simultaneously minimizing the number of radars in the network as a means of controlling the life-cycle costs of the system.

The increasing need for improved coverage at low altitudes, particularly in the planetary boundary layer, is articulated in several recent reports produced by federal agencies and National Research Council committees (e.g., NRC, 2002; NRC, 2004; NRC, 2008; NRC 2009; OFCM, 2006). These reports reflect the emerging need for improved low-altitude radar coverage to support numerous applications ranging from improved hazardous weather forecasting and warning, to wind mapping for fire fighting and tracking airborne toxic release, to monitoring bird migration, to enhanced support for roadway weather. Beyond weather, the DoD's Strategy for Homeland Defense & Civil Support (DoD, 2005, pg. 26) notes, "the nation will need to develop an advanced capability to replace the current generation of radars to improve tracking and identification of low-altitude threats." Such needs cannot be met with networks comprised of

long-range radars owing to the fundamental inability of such systems to provide comprehensive low-altitude coverage.

The National Science Foundation (NSF) Engineering Research Center (ERC) for Collaborative Adaptive Sensing of the Atmosphere (CASA) is researching a new weather hazard forecasting and warning technology based on low-cost, dense networks of radars that operate at short range, communicate with one another and adjust their sensing strategies in direct response to the evolving weather and to changing user needs (McLaughlin, et al. 2005; Kurose, et al. 2006; Philips et al. 2007). In contrast to the large weather radars in today's operational networks, such as NEXRAD having 9-meter diameter antennas and radar spacing of hundreds of kilometers, the antennas in dense networks are expected to be 1-meter in size with the radars spaced tens of kilometers apart. The small size of these radars allows them to be placed on existing infrastructure elements such as communication towers and rooftops (Figure 1). The short range of the radars defeats the earth curvature blockage problem, enabling these networks to comprehensively map damaging winds and heavy rainfall from the tops of storms down to the boundary layer beneath the view of today's networks. In addition to enabling comprehensive low-altitude observations, short-range operation offers the potential for significant improvements in resolution and update times compared to today's state-of-the-art. These improvements, in turn, enable a better characterization of storm morphology and analysis, offering the potential for improvements in weather hazard forecasting and warning. In addition to the radars and their associated hardware and data communication infrastructure, a new generation of meteorological software is being developed to target the resources in these radars to simultaneously support emergency managers and government and private industry organizations that need weather data for making critical decisions.

A dense network of ~10,000 such radars would be required to blanket the contiguous U.S. at 30 km radar spacing. Such radars would require less than 100 W of average transmitter power, yet they would be capable of mapping storms with < 1 km spatial resolution throughout the entire troposphere – from the critical low troposphere “gap” region up to the tops of storms. Such networks thus have the potential to supplement – or perhaps, replace – the large networks in use today. Blanket deployment of thousands of small radar nodes across an entire nation is but one of several possible future deployment strategies for this technology. Additional strategies would potentially include selective deployment of smaller networks in heavy population areas; in geographic regions particularly prone to wind hazards or flash floods; in valleys within mountainous regions; or in specific regions where it is particularly important to improve observation of low-level meteorological phenomena. Cost, maintenance, and reliability issues, as well as aesthetics and radiation safety concerns motivate the use of small (~1 meter diameter) antennas and low-power transmitters that could be installed on either low-cost towers or existing infrastructure elements (such as roof-tops or communication towers)<sup>3</sup>. The cost to deploy and operate a dense network will include both the up-front cost of the radars and the recurring costs to maintain them, buy or rent land and space on towers/rooftops, and provide for data communication between the radars, operations and control centers, and users. These costs, in addition to numerous technological and system-level tradeoffs, need to be balanced to ultimately develop an effective system design.

The CASA Engineering Research Center is a partnership among academic, industrial, and government participants ([www.casa.umass.edu](http://www.casa.umass.edu)). The center aims to lay the fundamental and technological foundations for dense, adaptive radar networks, conduct proof-of-concept

---

<sup>3</sup> The average equivalent isotropic radiated power (EIRP) of such radars would be 48 dBW, compared to 76 dBW for the WSR-88D radars. Given the FCC’s 1.0 mW/cm<sup>2</sup> microwave radiation safety specification, such small radars are radiation-safe at ranges beyond 20 m, whereas WSR-88D radiation safety begins at 530 m.

demonstrations using field-scale testbeds deployed in hazard-prone areas, and ultimately transition the concepts and technologies into practice through commercialization and technology transfer mechanisms. Projects undertaken within the center include the design and fabrication of low-power solid state radars, new hazard detection algorithms that make use of the data, and the creation of an open system software architecture for organizing hardware and software components and interfacing to multiple groups of data users. The first testbed, comprising a network of four small radars, was installed during winter/spring 2006 on telecommunication towers in southwest Oklahoma in a region frequented by tornadoes and severe thunderstorms. A user group comprised of emergency managers and public and private sector weather forecasters is included in the CASA team and is participating in the design and testing of the system.

This paper discusses key system-level tradeoffs associated with this new approach to weather radar network design and documents key aspects of CASA's first testbed deployment as a proof-of-concept. As background, we begin in Section 2 by characterizing the low-altitude "sensing gap" that limits the coverage of any network comprised of widely spaced radars, and we show how a dense network of closely-spaced radars overcomes this limitation. Placing radars close together (a few tens of km apart), and operating them as a network substantially reduces the radar physical size and transmitted power compared to today's weather radar designs. In Section 3 we describe the tradeoffs related to choice of wavelength, antenna size, power level, and radar spacing for this concept. Section 4 presents results from CASA's Oklahoma testbed network and highlights the collaborative, adaptive radar coordination system developed to support networked X-band radar operation. The approach to weather radar described in this paper is still being matured, and while the Oklahoma testbed trials look promising, additional work needs to be done to prove that this concept can be realized efficiently and effectively as a

new technology. Accordingly, Section 5 addresses cost issues, mentions some potential shortcoming of this approach, and discusses open issues that need to be further investigated. Pointers are also given to publications in the literature that describe aspects of this concept in greater detail. This paper concludes with Section 6.

## 2. Sensing Gap

Figures 2a and 2b show NEXRAD coverage at altitudes of 3 km (~10,000 ft) and 1 km (~3200 ft) above ground level (AGL), respectively (data courtesy I. Graffman, NOAA/NWS/OST; see also Maddox et al. 2002). Coverage at 3 km altitude is comprehensive east of the Rocky Mountains where the spacing between radars is ~230 km. In the western part of the country, where the representative spacing between radars is ~345 km, coverage gaps exist as a result of both earth curvature blockage and terrain blockage (NRC, 1995). Coverage is poor at 1 km altitude throughout the entire CONUS except in those regions in close proximity to the radar antennas.

The only way to provide more comprehensive coverage of the lower troposphere (e.g., < 3 km AGL) is to decrease the spacing between the radars. Figure 3 plots the percentage of the volume in a thin layer above ground level covered versus radar spacing for different altitudes (solid curves).<sup>4</sup> Also plotted is the number of radars needed for blanket CONUS coverage versus radar spacing (dashed line). The vertical bars in the figure at 230 km and 345 km are the two representative NEXRAD spacings discussed above. As shown in the plots, decreasing the spacing between the radars increases the low-altitude coverage (solid lines tending to increase toward 100% with decreasing radar separation); the blockage due to the earth's curvature is

---

<sup>4</sup> The curves are idealized, smooth earth approximations. The plots assume a lowest beam tilt angle of 0.5 deg; the minimum tilt angle for a NEXRAD radar. Increasing the minimum tilt angle shifts the curves to the left; the 0.9 deg minimum beam tilt angle for the radars in the CASA testbed network discussed in Section 3, for example, shift the breakpoint in the 300 m curve from ~50 km to ~30 km.

“defeated” when the radar spacing is reduced to ~50 km or less. The next section discusses the radar engineering tradeoffs that motivate consideration of small X-band radars spaced ~30 km apart, a spacing at which, as shown in Figure 3, ~10,000 radars would be required for complete CONUS coverage. The beamwidth for these radars will be about 1.8 degrees. As shown in Figure 4, the entire beam of such a radar at its lowest tilt of 0.9 degrees is below 1 km. The center of the beam is 0.5 km above ground level at 30 km; the worst-case beam height is lower than this value when the radars are operated in a network as we describe in Section 4.

### 3. Short-Wavelength Engineering Design Tradeoffs

Cost-effective deployment of dense networks comprised of large numbers of radars requires that the acquisition, deployment, and recurring costs be substantially smaller than the per-radar costs of today’s high-power radar designs. Rather than acquiring acre-sized land plots and deploying large towers to accommodate megawatt-class transmitters and 12-meter radomes, dense networks will require deployment on small towers having small land footprints or the utilization of existing infrastructure elements, such as rooftops, sides of buildings and communication towers. This requires that the radars be physically small and that the radiated power levels be low enough so as not to pose an actual or perceived radiation safety hazard.

A reasonable size for unobtrusive equipment deployment on existing infrastructure elements is an antenna aperture of 1-meter. The aperture size ( $d$ ) limits the resolution achieved by a radar according to the relationship,

$$resolution \text{ (km)} = beamwidth \text{ (radians)} \times range \text{ (km)} \quad (1)$$

where,

$$beamwidth \approx \lambda / d \quad (2)$$

Operating a radar having a 1-meter antenna at S-Band ( $\lambda = 10$  cm), the frequency of the WSR-

88D NEXRAD system, results in a beamwidth of 5.7 degrees, which corresponds to a 3 km spatial resolution at 30 km range<sup>5</sup>. However, sub-km scale weather features such as tornadoes cannot be resolved at this coarse resolution. By going to a shorter wavelength, the resolution can be improved. Operating the same 1-meter antenna at a wavelength of approximately 3 cm (X-band) reduces the beamwidth to 1.8 degrees for a spatial resolution of 1 km at 30 km range.<sup>6</sup>

Short-wavelength (X-band) operation has the benefit of attaining high spatial resolution with a smaller size aperture. Short-wavelength ( $\lambda \sim 3$  cm) operation also takes advantage of enhanced Rayleigh/Mie scattering from hydrometeors, but at a cost of increased attenuation in the presence of precipitation. Table 1 provides a comparison of attenuation at S-band to attenuation at the shorter X-band wavelengths (calculated as in Doviak & Zrnic, 1993, pg. 42). The large X-band attenuation values shown here preclude use of X-band for long-range radar designs, but it is practical to build an adequate margin for attenuation into the radar design when operating at tens of km range. Willie et al. (2006) estimated the actual attenuation that would be experienced as a function of range for X-band radars viewing springtime rainstorms in Oklahoma with results shown in Figure 5. Note that the data in the figure only include data collected during rainstorms. In particular, the curves show that radars designed for 30 km maximum range will experience two-way attenuation less than 16 dB for 90% of springtime rainstorms in Oklahoma.<sup>7</sup> The corresponding 90% value for radars designed for 60 km maximum range is 7 dB higher, at 23 dB. Such an analysis drives consideration of shorter (i.e., moving to

---

<sup>5</sup> The important figure-of-merit here is the resolution achieved in the cross-range (i.e., azimuth or elevation) direction, since this is the attribute of a radar's spatial resolution that is limited by the physical size of the antenna. Achieving high spatial resolution in the range direction is a relatively simple matter to achieve using modest radar receiver bandwidths.

<sup>6</sup> Signal-processing techniques similar to those being proposed for NEXRAD "super-resolution" (Torres and Curtis, 2006) can be applied to sharpen this resolution even further.

<sup>7</sup> The springtime is referred to as Oklahoma's "tornado season", with the majority of tornados occurring between March and May.

the left in Figure 5) rather than longer (i.e., moving to the right in the figure) separations and 30 km has been selected by the CASA project as a starting point for radar design.

Figure 6 combines the attenuation information of Figure 5 with the other variables needed to perform a standard radar range equation analysis to estimate the measurement sensitivity for radars deployed in networks with 30 km spacing as a function of radar transmitter power. The three curves describe the sensitivity that would be obtained at 30 km range under clear-air conditions (lowest curve; no attenuation) and during precipitation (middle and upper curves; attenuation data from Figure 5). The horizontal axis depicts average transmitted power levels ranging from several hundred milliwatts through 10W, through 100W. As a point of reference, 10W represents the average power emitted by a moderate-power magnetron transmitter. Such transmitters are small devices (approximately the size of a fist or a human heart) that cost under \$1000. 100 W represents an estimate of the power level that could be achieved using a low-cost phased array panel. Absent attenuation, the sensitivity at 30 km depicted in Figure 6 ranges between 10 dBZ and 0 dBZ for transmitter power levels between 10W and 100W, respectively.

#### **4. Networked Operation**

In current operational weather radar networks, radar coverage is non-overlapping (except at high altitudes) and the radars are operated largely independently of one another, repeatedly scanning the entire volume around the radar in a “sit-and-spin” fashion. In contrast, an essential feature of the short-range radars in the dense networks envisioned and described in this paper is to arrange them to have full overlapping coverage so that every location in the network is visible to multiple radars. This requires setting the maximum range of the radars approximately equal to

the spacing between the radars<sup>8</sup>. This permits the use of a radar control architecture that coordinates the beam scanning of the radars in the network both *collaboratively* – to obtain simultaneous views of a region for data fusion based algorithms such as multiple-Doppler wind field retrievals (discussed in this section) and network based attenuation correction (see Section 5) – and *adaptively* to optimize where and how the space over the network is scanned based on the type of weather occurring there and the data product needs of the system’s users. The result of this *collaborative adaptive sensing* approach is network level performance that exceeds the capabilities of its component radars in terms of update rate on key weather features, minimum beam height, spatial resolution, sensitivity, attenuation tolerance, and ability to support multiple users and multiple applications. Such network advantages – examples of which are demonstrated in this section – decrease the design requirements on the individual radars that make up the network. That is, key radar size and cost drivers, such as the antenna size and the peak transmitter power needed to achieve a particular level of resolution or sensitivity, are lower than they would need to be if the radars were not part of a collaborative, adaptive network. This concept, which CASA has implemented as a “Meteorological Command and Control” (MCC) software architecture in its “IP1” (Integrative Project #1) demonstration network in Oklahoma, is one of the core enabling technologies behind the dense network approach. This section motivates the collaborative, adaptive sensing concept of radar operations, describes the IP1 demonstration network, and gives some examples from the network to illustrate the potential advantages of the dense network collaborative, adaptive sensing approach.

---

<sup>8</sup> Covering the cone-of-silence above a radar requires that the maximum range be set slightly higher than the radar spacing. This is described in greater detail in (McLaughlin et al. 2007). This spacing rule is satisfied by the WSR-88D network in the eastern part of the CONUS, enabling that system to achieve a degree of overlapping coverage at higher altitudes (e.g., > 3 km).

### *a. Collaborative, Adaptive Sensing*

Under a traditional sit-and-spin concept-of-radar-operations, the update rate is the same for all locations covered by the radar network. As the number of elevation angles required to cover the volume of interest increases, however, this update rate can become unacceptably long.<sup>9</sup> On the other hand, it is not necessary to scan all meteorological phenomena at same update rate or in the same way. Powerful supercells within which circulations are rapidly forming and dissipating should be sampled at a much higher rate and with a different scan strategy than, for example, a large-scale, slow-moving stratiform rain event. Working with users of weather radar data – National Weather Service forecasters, emergency managers, and a variety of subject matter experts – CASA has identified update rates and scan strategies for different types of weather phenomena (Philips et al. 2008). To execute these user defined scan strategies the MCC in the IP1 demonstration network employs a concept-of-radar-operations based on *targeted sector scanning*. That is, instead of the radars sitting-and-spinning, the radars perform back-and-forth, bottom to top raster scans of selected sub-volumes of the network at update rates that depend on the weather features detected in the volumes. Through such a time-space adaptive, targeted sector-scanning approach the network achieves update rates on the order of 1-minute of those weather features that the system's users have indicated are most important to their data needs. In addition, by optimally selecting which radar(s) are used to scan a given sub-volume, the MCC is able to achieve a network-level performance that is better than that of the individual radars that make up the network. In particular, for the IP1 demonstration network where the radars are arranged approximately as equilateral triangles of 30 km on a side (as will be

---

<sup>9</sup> In general, the shorter the operating-range of a radar, the larger the number of elevation angles required to meet a given coverage ceiling requirement. For example, for volume coverage up to 21 km (the coverage ceiling requirement for the current NEXRAD system) the radars in a dense network with 30 km radar spacing would have to cycle through nearly 30 elevation angles. NEXRAD, in contrast, cycles through no more than 14 elevation angles for sit-and-spin volume update rates of between 4 and 5 minutes.

described shortly), a simple “choose the closest radar” strategy means that no point in the network is farther than  $\sim 18$  km from a radar.<sup>10</sup> For range dependent performance metrics such as minimum beam height above ground level and spatial resolution this leads to a *network improvement factor* of approximately 40% over the performance at 30 km. Thus, radars whose beam center and spatial resolution at 30 km are 500 m and 1 km, respectively, achieve beam floor and spatial resolution levels no more than 300 m and 600 m, respectively in a network. For performance metrics that depend on the square of the range such as sensitivity, the network improvement is nearly 65%, or 4.4 dB. Thus, radars having 10 dBZ sensitivity at 30 km achieve worst-case sensitivity of no more than 6.6 dBZ under networked operation. For the case where the closest radar might be attenuated, e.g., due to severe radome wetting or due to intense precipitation between the closest radar and the volume of interest (recall Table 1), a “choose the least attenuated radar” strategy can be used. The network advantage under such a strategy can be a dramatic reduction in the path attenuation a radar needs to overcome. The study in (Chandrasekar et al. 2009b) shows a reduction in the 90% attenuation margin of almost 10 dB under networked operation.<sup>11</sup> In addition to the advantages above, by choosing multiple radars to simultaneously scan a common volume one obtains the additional advantage of being able to extract data products not easily or as accurately obtained from single radar measurements, such as the simultaneous measurement of several linearly independent components of the wind for 2- and 3-D wind field estimation (multiple-Doppler wind field retrieval), or the estimation of reflectivity from multiple observations of a common volume along differently attenuated paths (Chandrasekar and Lim, 2008). The targeted sector scan approach used by the IP1 MCC is

---

<sup>10</sup> 18 km is the distance to the center of an equilateral triangle with side lengths equal to 30 km.

<sup>11</sup> Technically, the range related performance improvements hold for all points in the network except the fraction of its volume due to the cone-of-silence above each radar. Here overlap is sufficient for a neighbor to cover this region, but there will be no range related network improvement over a radar’s baseline performance at a range equal to the spacing of the radars in the network. However, even for the cone-of-silence regions there can be a reduction in “effective” attenuation and improvement in velocity vector accuracy with judicious choice of which radar(s) perform the scan.

discussed in more detail below. For more rigorous treatments of the principles and advantages network based sensing cf (Junyent and Chandrasekar, 2009; Chandrasekar et al. 2004; Chandrasekar and Jayasumana, 2001; Insanic and Siqueira, 2008).

### ***b. Demonstration Network***

To investigate the dense network paradigm and collaborative adaptive sensing concept, the participants of the CASA project designed, fabricated, and deployed a four-radar testbed in Oklahoma. This IP1 demonstration network covers a 7,000 square km region in southwestern Oklahoma that receives an average of 4 tornado warnings and 53 thunderstorm warnings per year (Brotzge, 2006). The radars are spaced approximately 30 km apart and arranged in a topology consisting of back-to-back equilateral triangles, an arrangement chosen because it maximizes the volume of atmosphere around the network satisfying the conditions for dual-Doppler velocity vector retrievals (Brewster et al. 2005). The maximum ranges of the radars are set to 40 km to provide the overlapping coverage needed for multiple radar measurements and collaborative, adaptive scanning experiments, including the ability of a radar to cover the cone-of-silence of each of its neighbors. Figure 7 shows the radars in the IP1 testbed along with their coverage range rings. Also shown in the figure are the two nearest NEXRAD radars, KFDR at Frederick to the southwest and KTLX at Twin Lakes to the northeast. The range rings around these radars at 40 km and 60 km respectively show that the IP1 network is essentially midway between these two radars in the low-level coverage gap between them. From a larger network perspective, IP1 represents two unit deployment cells in the sense that deployment of larger numbers of radars covering larger spatial domains would be made by replicating the triangular topology shown in Figure 7.

Figure 8 shows the architecture and major subcomponents of the individual radars in the network (Junyent, 2007; Junyent et al. 2005). These radars are small-size (1.2 m parabolic dish antenna), short-wavelength (3.2 cm, 9.41 GHz, X-band) units. Using low-power magnetron transmitters (10 kW peak, 13 W average<sup>12</sup>), they have a single-pulse sensitivity of 10.8 dBZ<sub>h</sub> at 30 km. The radars provide dual-polarization capabilities (simultaneous linear horizontal and vertical) (Bringi and Chandrasekar, 2001) with a dual-polarized waveguide/antenna feedhorn assembly and dual-channel coherent-on-receive receiver/data acquisition system (Khasgiwale et al. 2005). To facilitate targeted sector scanning, the radars sit atop a high performance pedestal assembly capable of high accelerations and rapid back-and-forth PPI (plan-position indicator) sector scanning. A linear actuator attached directly to the antenna provides movement in elevation, including an ability for rapid RHI (range-height indicator) scans. Except for replacing broken parts, the radars can be monitored, maintained, and operated remotely over the Internet. All data transfer from the radars is also by Internet links. For perspective, Table 2 compares an IP1 node to a WSR-88D NEXRAD node. CASA's costs to build and operate this network are discussed Section 5 of this paper.

Running in a UNIX based computer at each radar is an integrated suite of algorithms for signal processing (short-wavelength range-velocity ambiguity mitigation and attenuation correction, low-level clutter suppression) and polarimetric meteorological moment data estimation (Cho et al. 2005). Table 3 lists the data products generated by the IP1 radars. For velocity ambiguity mitigation, a dual-PRF waveform unfolds Doppler velocities up to  $\pm 38$  m/s (Bharadwaj and Chandrasekar, 2005). For range ambiguity mitigation, an algorithm based on the random phase coding naturally provided by the magnetrons (Siggia, 1983) suppresses up to 20

---

<sup>12</sup> This is the total radiated power. The IP1 radars are SHV dual-pol radars putting out 5.0 kW peak power per polarization. The duty cycle of the IP1 radars for its dual-PRF "storm" waveform is 0.13%, or 6.5 kW average radiated power per-polarization.

dB of overlaid echoes (Bharadwaj and Chandrasekar, 2007). The algorithms for clutter suppression and attenuation correction are discussed in Section 5. Figure 9 from the IP1 radar at Cyril (KCYR) shows the dual-polarization products reflectivity ( $Z_h$ ), differential reflectivity ( $Z_{dr}$ ), differential phase ( $\phi_{dp}$ ), and correlation coefficient ( $\rho_{hv}$ ) resulting after ambiguity mitigation, clutter suppression, and attenuation correction.

### ***c. Meteorological Command and Control***

Collaborative, adaptive sensing in the IP1 network is accomplished using a *Meteorological Command and Control* (MCC) software architecture. As shown in Figure 10, this architecture “closes-the-loop” between sensing and radar control; the top part of the loop corresponds to data ingest, the bottom part of the loop corresponds to radar control. To explain, we walk through the five major steps listed in the figure. The first step is the ingest of the data products from the four radars into a data repository. This involves sending the data products produced by the IP1 radars in the field, over the Internet, to a System Operation and Control Center (SOCC)<sup>13</sup>. The SOCC performs functions of archival and real-time dissemination of data to users. In addition, as data arrives at the SOCC, weather detection algorithms in Step 2 are run on it in real-time to identify the locations of significant weather features within the radar network domain. For IP1 these currently include algorithms for reflectivity contouring, storm cell identification, and circulation detection. In Step 3, the detections from the weather detection algorithms are posted in a feature repository. While Figure 10 only shows data coming from the IP1 radars, the feature repository can accept detections from other sources, including, for example, NEXRAD or manually entered storm-spotter reports. The process of radar control begins in Step 4, where the detected weather features are converted into abstractions called tasks.

---

<sup>13</sup> The SOCC can physically be located wherever there is an adequate network connection. The IP1 system is typically operated from a SOCC installed in an office in the National Weather Center in Norman, OK.

In simple terms, a task is a sub-volume of the atmosphere identifying where significant weather features are located within the network coverage domain, a classification as to whether or not the feature is associated with strong winds or high reflectivity, and a user assigned value indicating how important it is to scan the task within the next minute. Since there are generally many tasks (i.e., many weather features of potential interest) in the network at any time, an optimization process in Step 5 applies a scanning strategy that is a combination of the “pick closest radar/pick least attenuated radar” discussed previously, trading off factors such as the sector sizes to be scanned (in azimuth and elevation) against closeness, signal-to-noise ratio (SNR), the number of tasks to be scanned, the past history of scans, and the values assigned to the tasks by the users of the system (Pepyne et al. 2008; Zink et al. 2008b). The actual commands output from the MCC to the radars are described next.

#### ***d. Performance Examples***

Since the first multi-radar data was ingested from the IP1 network on 9 May 2006, several terabytes of data has been collected and analyzed. This includes evaluation by NWS forecasters in the NOAA Hazardous Weather Testbed at the National Weather Center in Norman OK during two Oklahoma spring storm seasons (2007 and 2008). For these experiments, the MCC operated as follows: Scanning was divided into 1-minute intervals (referred to as MCC “heartbeats”). During each such 1-minute heartbeat, each radar performed a low-level 360 PPI surveillance sweep at 2 degrees (20 sec) followed by a multiple elevation PPI sector scan targeted on one or more important meteorological phenomenon (40 seconds)<sup>14</sup>. The orientation and width of the sector in azimuth was determined by the MCC optimization (Step 5 in Figure 10) to cover the meteorological features of interest to the users, while the number of elevations

---

<sup>14</sup> Periodically the radars also do a 10 second RHI scan for storm vertical cross-section analysis and storm top finding. When an RHI is performed, the time for PPI sector scanning is reduced from 40 to 30 seconds.

scanned within the sector varied with the width of the sector. For example, a 60-degree sector included 7 elevations, while a 180-degree sector included only 4 elevations. The elevation angles used were 1, 3, 5, 7, 9, and 11 degrees for coverage from less than 600 m to more than 10 km above ground level. Figure 11 illustrates this combined surveillance and multiple-elevation sector scan strategy. The right side of the figure shows a merged composite reflectivity product of surveillance scans taken of a rapidly evolving supercell with an appendage from an April 10, 2007 severe weather event.<sup>15</sup> The left side of the figure shows a multiple-elevation sector scan targeted on the appendage, revealing the details of its vertical structure. Both the merged image and the multiple-elevation sector scans can be viewed simultaneously and both are updated each minute as the MCC optimizes radar scans in real-time. The high resolution and fast updates offered by a dense network are illustrated in Figure 12, which compares observations of a hook echo from the IP1 radar at Lawton to observations of the same event from the nearest NEXRAD radar at Fredrick (KFDR). The short-range operation and narrow sector scanning detects fine scale features at 200 m altitude that are not visible in the WSR-88D observations and the targeted sector scanning offers update rates 5 times faster on the important weather features (Brotzge et al. 2008). For scanning those volumes of the network visible to multiple-radars, the IP1 MCC was designed with a scan optimizer for properly coordinating multiple radars to generate multi-Doppler scans of detected storm cells for multi-Doppler wind field retrieval (Wang et al. 2008). Figure 13 shows examples of the resulting wind vector products from the system; algorithms for generating similar wind-vectors in near real-time are being tested (Gao et al. 2008).

Space constraints have only allowed us to illustrate a few examples of the advantages provided by the dense network and collaborative adaptive sensing concepts, but it is becoming clear that the dense network concept is demonstrating performance that goes well beyond the

---

<sup>15</sup> For this appendage CASA has visual confirmation of a funnel cloud from a television station storm spotter video.

current NEXRAD operational state of the art in terms of temporal and spatial resolution, low-altitude coverage, and ability to observe Doppler wind vector fields. A movie showing the IP1 MCC in action can be found at the CASA website (<http://casa.umass.edu/>).

## **5. Open Issues**

This section considers cost and phased-array technology for small radars. We also discuss some potential limitations of the small radar network approach, and we summarize some of the ongoing research projects aimed at maturing the concept.

### ***a. Cost***

Radars can be purchased today at prices ranging from \$200 for automobile collision radar, to \$2k-\$20k for marine navigation radars, to \$1M - \$10M for large weather radars, to costs in excess of hundreds of millions of dollars for the high-performance radars developed for complex missions in defense and other applications. The cost of a radar is driven both by the volume of radars manufactured and the required performance. The small radars considered for dense networks transmit  $< 100$  W average microwave power. From the point of view of transmitted power this puts them in the same performance category as the marine radars at the lower end of the price range, and if an opportunity develops to manufacture them in the large numbers envisioned in this paper, we anticipate the price to be in \$200k range<sup>16</sup>. While this number is admittedly speculative, CASA's costs to build, install, and operate the radars in the IP1 testbed serves as a useful first data-point in projecting costs for this new class of radar. The IP1 radars were designed and fabricated by CASA's academic participants during 2004-2005 using a combination of off-the-shelf and custom-made components (Junyent, 2007; Khasgiwale

---

<sup>16</sup> \$200k is a cost target set by the participants of the CASA project based on both a technology costing exercise and the following calculation: The 156 radar NEXRAD system cost \$1.56 billion to deploy between 1990 and 1997 (OFCM, 2006); assuming a \$2 billion cost to acquire and deploy 10,000 radars for use in a nationwide "blanket deployment" across the CONUS, the per-radar cost would need to be \$200k.

et al. 2005). The total parts-cost of the transceiver, antenna, computers, and data acquisition system for these dual-polarized, coherent-on-receive radars was \$78k. The total parts-cost, listed in Table 4, for all components in a complete installation, including the towers, concrete, radomes, environmental and power conditioning, and high-speed antenna positioners was \$229,500<sup>17</sup>. With two years of operating experience, CASA's annual operations and maintenance costs, also listed in Table 4, for each radar is \$26k. Several caveats are noted: the IP1 radars were developed by an academic team for use as an experimental research facility, and cost-containment was not a strong design driver in realizing this system; these numbers reflect parts-costs only, and they exclude labor and other costs associated with manufacturing and selling commercial products; moreover these represent low volume costs, given that the CASA project produced only four radars for this testbed.

#### ***b. Phased Array Radars***

Phased arrays are a key enabling technology in many radars produced for defense applications today, and they are a desirable technology for use in dense radar networks since they do not require maintenance of moving parts, they permit flexibility in beam steering without requiring heavy antenna pedestals such as those used in the CASA IP1 design, and they are more robust with respect to component failure.<sup>18</sup> Moreover, phased arrays can potentially be mounted to the sides of towers and buildings as shown in Figure 14 giving flexibility in the selection of suitable radar sites.

---

<sup>17</sup> One of the four radar installations cost \$80k more than this figure, owing to the construction of a taller, larger capacity tower.

<sup>18</sup> Radar uptime for the 7-week 2007 spring storm season was 93%. For the 9-week 2008, the uptime percentage was 94%. In fact our biggest reliability problems with IP1 have been with the magnetrons and associated modulator boards, both single point failures. We admit that this is partially a result of our pushing the capabilities of these low cost transmitters with dual-PRF waveforms and so on, but it also points to the desirability of solid-state radars with their property of "graceful degradation" with array element failure.

A particular challenge to realizing cost-effective dense networks comprised of thousands of phased-array radars will be to achieve a design that can be volume manufactured for ~\$50K per phased-array panel (assuming 4 panels per site and assuming each panel is a self-contained unit containing the antenna elements and radar transceivers as well as computers for beam steering, data acquisition, and signal processing, communication interfaces and power conditioning electronics). Establishing the specifications for these arrays is currently a work-in-progress (e.g., McLaughlin et al. 2007); however several key parameters can be stated as listed in Table 5.

Several thousand transmit/receive (T/R) modules are needed to obtain a phased array capable of electronically steering a 2-degree beam in two dimensions over the desired scan range without requiring moving parts. Realizing such an antenna requires the use of low-cost microwave semiconductors combined with very low-cost packaging, fabrication and assembly techniques. Puzella and Alm (2007) and Sarcione et al. (2008) describe an architecture and prototype of a phased array with these characteristics being developed by Raytheon based on manufacturing processes similar to those for making low-cost computer boards. Another approach to realizing these panels is to perform electronic beam steering in the azimuth direction while mechanically steering (tilting) the antenna in the elevation direction. Salazar et al. (2008) describe a prototype version of such an antenna being developed within the CASA center. Since electronic beam steering is only needed in the azimuth direction, the individual panels in this design require only 64 1-Watt T/R modules, each of which is estimated to cost \$500, which, when realized, is expected to result in a cost of less than \$50k per panel (McLaughlin, 2008).

### ***c. Potential Limitations***

While this paper argues that dense networks of small radars have the potential to supplement, or perhaps replace, large radars, it is recognized that the concept proposed here is still a research work-in-progress, and it may ultimately not prove feasible to do all the types of measurements that large radars can perform. Two specific examples where large radars will outperform small radars are in achieving sensitivity to weak echoes and performing observations over the ocean. In those regions where they have visibility (e.g., above 2-3 km AGL) large, high-power radars are capable of achieving higher sensitivity than the small radars described here. Large radars sited near the coast have the ability to observe atmospheric flows as much as 200 km from the shoreline; this will not be feasible with smaller short-range radars installed on land-based sites.

### ***d. Ongoing Research Projects***

There are a number of signal processing challenges that need addressing in order to effectively operate small, low power, short wavelength radars at low elevation angles. Attenuation and clutter are two such challenges. Even operating at short-range, attenuation introduces errors into estimates of reflectivity that must be accounted for. A dual-polarization attenuation correction is currently employed in IP1 to correct the retrieved radar reflectivity and differential reflectivity in real time (Lim and Chandrasekar, 2005; Lim et al. 2007; Liu et al. 2007). Its performance is demonstrated in Figure 15a, with comparison against NEXRAD observations. Using the capability for simultaneous measurements from multiple radars, a network-based attenuation correction algorithm has also been devised in CASA (Chandrasekar and Lim, 2008). This algorithm, which involves the simultaneous solution of a set of integral equations describing the backscatter and propagation properties of a common observation

volume, brings the new paradigm of network based processing, and is being evaluated for real-time operation in the IP1 network. To separate ground clutter from weather echoes, various clutter suppression techniques are being explored. The current technique, whose performance is illustrated in Figure 15b, is a spectral based approach that suppresses up to 40 dB of clutter contamination (Moisseev and Chandrasekar, 2008; Moisseev, Nguyen, and Chandrasekar, 2008). Similar in design to GMAP (Siggia and Passarelli, 2004) the algorithm does not require a clutter map; a property particularly useful under the IP1 targeted sector scan approach. Other techniques are being evaluated, including some of which may more suitable for phased-array radar applications (Nguyen, Moisseev, and Chandrasekar, 2008).

A potentially rich application for dense network technology is hydrological forecasting in complex terrain where long-range radars cannot see due to terrain blockage. After several years of in-house study, Meteo-France, for example, has chosen to install 2-4 gap-filling X-band radars in the Tinee and Ubaye river valleys along the French eastern boarder to improve hydrological forecasts and flood warning there (Tabary et al. 2008). For QPE, CASA is exploring the use of the specific differential propagation phase ( $K_{dp}$ ). Not only does  $K_{dp}$  have higher sensitivity at X-band compared to the low-attenuating frequencies (C and S-band) but it is relatively immune to rain attenuation, calibration biases, partial beam blockage, and hail contamination. See (Chandrasekar, Maki, Wang, and Nakae (2009a) for preliminary results on the capabilities and potential of X-band dual-polarization radar networks for flood warning in urban settings where building clutter is an issue.

Controlling, monitoring, assimilating, and disseminating data from 10,000 radars promises to be a major challenge. For radar control in large networks, distributed versions of the MCC described in Section 4 have been developed where each radar runs a separate MCC and the

MCC's negotiate with their nearest neighbors to decide which radar(s) should scan each task and how the scan should be performed (Kranin, An, and Lesser, 2007). For remote monitoring and management the radars in the IP1 testbed are all Internet accessible and the radar software has been configured with various scripts for remote testing and calibration. For getting data to and from the radars, wireless links to the radars, compression schemes for the data, and techniques for needs-based data transmission are being explored (Li et al. 2007).<sup>19</sup> For integration with the existing infrastructure, CASA has made its data products compatible with existing NWS formats (NetCDF etc.) and existing NOAA/NWS/EM visualization tools such as WDSS-II (Lakshmanan et al. 2007) and WeatherScope (<http://climate.ok.gov/software/>). For Internet operation, CASA has also developed its own custom web-based visualizations, and is working on visualizations for handheld devices for individuals such as emergency managers, tornado spotters, and first responders to use in the field.

Other research within CASA is evaluating the dense network concept through an analysis of the IP1 data. (Brotzge et al. 2007; Chandrasekar et al. 2008) report on the overall operation of the network. Zink et al. (2008a) evaluate the performance of the MCC. (Bharadwaj, Chandrasekar, and Junyent, 2007) evaluate the IP1 signal processing waveforms. Data assimilation from CASA is addressed in (Brewster et al. 2008). (Philips et al. 2008) reports on studies related to identification of user need and user experience with the collaborative adaptive sensing paradigm. Analysis of IP1 tornado detection and forecasting with CASA networks is reported in (Brotzge et al. 2008; Brotzge et al. 2009; Chandrasekar et al. 2007; Proud et al. 2008; Potvin et al. 2007).<sup>20</sup> The impact of IP1 data on numerical weather prediction (NWP) is explored

---

<sup>19</sup> Estimating the meteorological moments at the radars themselves, rather than shipping the I, Q data from the radars for such estimation, is equivalent to about a 100:1 compression ratio over the raw radar data.

<sup>20</sup> During the 2007 spring experiment two confirmed tornadoes occurred within the coverage domain of the IP1 testbed. However, despite a record number of tornadoes in the U.S. in 2008, none occurred in the IP1 testbed domain. The IP1

in (Schenkman et al. 2008). (Cheong et al. 2008) reports on refractivity measurements conducted at X-band for obtaining low-level moisture fields with such networks.

## **6. Summary**

Current approaches to operational weather observation are based on the use of physically-large, high-power long-range radars that are blocked from viewing the lower part of the troposphere by the earth's curvature. This paper describes an alternate approach based on dense networks comprised of large numbers of small X-band radars. Spacing these radars tens of km apart defeats the earth curvature problem and enables sampling the full vertical depth of the atmosphere using 1-m antennas and transmitters having only 10's of W transmitter power. Such networks can provide observing capabilities beyond the operational state of the art while simultaneously satisfying the needs of multiple users. Improved capabilities associated with this technology include low-altitude coverage, sub-km spatial resolution, rapid update times, and multi-Doppler retrievals of vector winds. This technology has the potential to supplement, or perhaps replace, the widely spaced networks of physically large high power radars in use today.

## **Acknowledgements**

This work is supported primarily by the Engineering Research Centers Program of the National Science Foundation under NSF award number 0313747. Any opinions, findings, conclusions, or recommendations expressed in this material are those of the authors and do not necessarily reflect those of the National Science Foundation. CASA is a consortium of Academic, Government, and Industry partners including the University of Massachusetts at Amherst (lead organization), University of Oklahoma, Colorado State University, University of Puerto Rico at Mayaguez, University of Delaware, University of Virginia, Rice University, McGill University,

---

testbed detected both of the 2007 tornadoes.

NOAA/National Weather Service, Department of Energy, OSHRE/OneNet, Raytheon Company, Vaisala Inc., IBM, DeTect Inc., EWR Weather Radar, WeatherNews International, KWTV/NEWS 9, and the Japan National Research Institute for Earth Science and Disaster Prevention (NIED).

## References

- Bharadwaj, N. and V. Chandrasekar, 2005: Waveform design for CASA X-band Radars. Preprints, *32<sup>nd</sup> Conf. on Radar Meteorology*, Albuquerque, NM, Amer. Meteor. Soc.
- Bharadwaj, N. and V. Chandrasekar, 2007: Phase coding for range ambiguity mitigation in dual-polarized Doppler weather radars. *J. Atmos. Oceanic Technol.*, **24**, 1351-1363.
- Bharadwaj, N., V. Chandrasekar, and F. Junyent, 2007: Evaluation of first generation CASA radar waveforms in the IP1 testbed. Preprints, *IEEE International Geoscience and Remote Sensing Symposium (IGARSS)*, Barcelona, Spain.
- Brewster, K. A., J. Brotzge, K. W. Thomas, Y. Wang, M. Xue, J. Gao, and D. Weber, 2008: High resolution assimilation of CASA and NEXRAD radar data in near-real time: Results from spring 2007 and plans for spring of 2008. Preprints, *12th Conference on IOAS-AOLS*, Amer. Meteor. Conf., New Orleans, LA.
- Brewster, K., L. White, B. Johnson, and J. Brotzge, 2005: Selecting the sites for the CASA NetRad, a Collaborative Radar Network. Preprints, *Ninth Symp. on Integrated Observing and Assimilation Systems for the Atmosphere, Oceans, and Land Surface (IOAS-AOLS)*, San Diego, CA, Amer. Meteor. Soc.
- Bringi, V.N. and V. Chandrasekar, 2001: *Polarimetric Doppler weather radar: Principles and Applications*. Cambridge University Press, 636 pp.
- Brotzge, J., 2006: Severe weather climatology of IP1. *CASA Technical Report*, Oklahoma University, OK. [Available from J. Brotzge, University of Oklahoma, 120 David L. Boren Blvd., Norman, OK 73072-7309].

- Brotzge, J., D. Andra, K. Hondl, and L. Lemon, 2008: A case study evaluating Distributed, Collaborative, Adaptive Scanning: Analysis of the May 8th, 2007, minisupercell event. Preprints, *Symposium on Recent Developments in Atmospheric Applications of Radar and Lidar*, AMS Conf., New Orleans, LA.
- Brotzge, J., K. Brewster, V. Chandrasekar, B. Philips, S. Hill, K. Hondl, B. Johnson, E. Lyons, D. McLaughlin, and D. Westbrook, 2007: CASA IP1: Network operations and initial data. Preprints, *23<sup>rd</sup> Conf. IIPS*, San Antonio, TX, Amer. Meteor. Soc.
- Brotzge, J., K. Hondl, B. Philips, L. Lemon, E. Bass, D. Rude, and D. Andra, Jr., 2009: Evaluation of Distributed Collaborative Adaptive Sensing for detection of low-level circulations and implications for severe weather warning operations. *Wea. Forecasting*, in review.
- Chandrasekar, V. and A. P. Jayasumana, 2001: Radar design and management in a networked environment. Preprints, *Proc. of ITCOMM*, Denver, CO, 142-147.
- Chandrasekar, V. and S. Lim, 2008: Retrieval of reflectivity in a networked radar environment. *J. Atmos. Oceanic Technol.*, **25**, 1755-1767.
- Chandrasekar, V., S. Lim, N. Bharadwaj, W. Li, D. McLaughlin, V.N. Bringi, and E. Gorgucci, 2004: Principles of Networked Weather Radar Operation at Attenuating Frequencies. Preprints, *Proc. of the 2004 European Radar Conf. (ERAD 2004)*, Visby, Sweden, 109-114.
- Chandrasekar, V., M. Maki, Y. Wang, and K. Nakane, 2009a: Considerations for Urban Flood Monitoring using X-band dual-polarization radar network. Preprints, *23<sup>rd</sup> Conf. on Hydrology, Special Symp. on Urban High Impact Weather*, 11-15 January, Phoenix, AZ, Amer. Meteor. Soc.

Chandrasekar, V., D. McLaughlin, J. Brotzge, M. Zink, B. Philips, and Y. Wang, 2007:

Distributed Collaborative Adaptive Radar Network: The CASA IP-1 Network and Tornado Observations. Preprints, *33rd Conf. Radar Meteorology*, Amer. Meteor. Soc., Cairns, Australia.

Chandrasekar, V., D.J. McLaughlin, J. Brotzge, M. Zink, B. Philips, and Y. Wang, 2008:

Distributed Collaborative Adaptive Radar Network: Preliminary Results from the CASA IP1 Testbed. *Proc. of the IEEE Radar Conference (RADAR'08)*, 26-30 May, Rome, Italy, 1-5.

Chandrasekar, V., D. Willie, Y. Wang, S. Lim, and D. McLaughlin, 2009b: Attenuation Margin

Requirements in a Networked Radar System for Observation of Precipitation. To appear, *IGARSS 2009: IEEE International Geoscience & Remote Sensing Symposium*, Cape Town, Africa, July 13-17.

Cheong, B., R. Palmer, C. Curtis, T. Yu, D. Znic, and D. Forsyth, 2008: Refractivity results

using the Phased-Array Radar: First results and potential for multimission operation. *IEEE Trans. On Geoscience and Remote Sensing*, **46**, 2527-2537.

Cho, Y.-G., N. Bharadwaj, V. Chandrasekar, M. Zink, F. Junyent, E. Insanic, and D.J.

McLaughlin, 2005: Signal processing architecture for a single radar node in a networked radar environment (NetRad). Preprints, *Proc. of the IEEE Int. Geoscience and Remote Sensing Symp. (IGARSS)*, Seoul, Korea.

DoD, 2005: Strategy for Homeland Defense and Civil Support. U.S. Department of Defense,

Washington D.C., (<http://www.defenselink.mil/news/Jun2005/d20050630homeland.pdf>).

Doviak, R. J. and D. S. Znic, 1993: *Doppler Weather Radar Observations* (2<sup>nd</sup> ed.). Dover

Publications, Inc., 562 pp.

- Gao, J., K. Brewster, Y. Wang, K. Thomas, J. Brotzge, and M. Xue, 2008: High-resolution three-dimensional wind analysis of CASA IP-1 and WSR-88D radar data using the ARPS 3DVAR. Preprints, *12<sup>th</sup> Conf. on IOAS-AOLS*, New Orleans, LA, Amer. Meteor. Soc.
- Insanic, E., and P. Siqueira, 2008: Resource allocation and optimization for a closely coordinated network of X-band radars. Preprints, *Proc. of the IEEE Int. Geoscience and Remote Sensing Symp. (IGARSS)*, Boston, MA.
- Junyent, F., 2007: Networked weather radar system using coherent-on-receive technology. *Ph.D. Dissertation, Dept. of Electrical and Computer Engineering*, University of Massachusetts, Amherst, MA.
- Junyent, F. and V. Chandrasekar, 2009: Theory and characterization of weather radar networks. *J. Atmos. Oceanic Technol.*, Amer. Meteor. Soc., in press.
- Junyent, F., V. Chandrasekar, D. J. McLaughlin, S. Fraiser, E. Insanic, R. Ahmed, N. Bharadwaj, E. Knapp, L. Krnan, and R. Tessier, 2005: Salient features of radar nodes of the first generation NetRad system. Preprints, *Proc. of the IEEE Int. Geoscience and Remote Sensing Symp. (IGARSS)*, Seoul, Korea.
- Khasgiwale, R., L. Krnan, A. Perinkulam, and R. Tessier, 2005: Reconfigurable data acquisition system for weather radar applications. Preprints, *48<sup>th</sup> Midwest Symp. on Circuits and Systems*, Covington, KY.
- Krainin, M., B. An, and V. Lesser, 2007: An application of automated negotiation to distributed task allocation. Preprints, *Proc. of the Int. Conf. on Intelligent Agent Tech.*, Silicon Valley, CA.

Kurose, J., E. Lyons, D. McLaughlin, D. Pepyne, B. Philips, D. Westbrook, and M. Zink, 2006:

An end-user responsive sensor network architecture for hazardous weather detection, prediction, and response. Preprints, *Asian Internet Eng. Conf. (AINTEC)*, Pathumthani, Thailand.

Lakshmanan, V., T.M. Smith, G.J. Stumpf, and K.D. Hondl, 2007: The Warning Decision

Support System – Integrated Information. *Weather and Forecasting*, **22**, 596-612.

Leone, D.A., R.M. Endlich, J. Petriceks, R.T.H. Collis, and J.R. Porter, 1989: Meteorological

considerations used in planning the NEXRAD network. *Bull. Amer. Meteor. Soc.*, **70**, 4-13.

Li, M., T. Yan, D. Ganesan, E. Lyons, P. Shenoy, A. Venkataramani, and M. Zink, 2007: Multi-

user Data Sharing in Radar Sensor Networks. Preprints, *Proc. of the 5th ACM Conference on Embedded Networked Sensor Systems (Sensys 2007)*, Sydney, Australia.

Lim, S. and V. Chandrasekar, 2005: An improved attenuation correction algorithm using dual-

polarization radar observations of precipitation. Preprints, *Proc. of Intl. Symp. on Geoscience and Remote Sensing*, Seoul, Korea, 25-29 July, IEEE.

Lim, S., V. Chandrasekar, P. Lee and A. P. Jayasumana, 2007: Reflectivity retrieval in a

networked radar environment: Demonstration from the CASA IP1 radar network. Preprints, *Proc. of the 27<sup>th</sup> IEEE International Geoscience and Remote Sensing Symposium (IGARSS)*, Barcelona, Spain.

Liu, Y., Y. Wang, D. Willie, V. Chandrasekar, and V. N. Bringi, 2007: Operational evaluation of

the real-time attenuation correction System for CASA IP1 testbed. Preprints, *33<sup>rd</sup> Conf. on Radar Meteorology*, Cairns, Queensland, Amer. Meteor. Soc.

- Maddox, R. A., J. Zhang, J. J. Gourley, and K. W. Howard, 2002: Weather radar coverage over the contiguous United States. *Wea. Forecasting*, **17**, 927-934.
- McLaughlin, D. J., 2008: *CASA Update for NEXRAD TAC*. Briefing to the NEXRAD Technical Advisory Committee, September 4, 2008, MIT Lincoln Laboratory, Lexington, MA.
- McLaughlin, D. J., V. Chandrasekar, K. Droegemeier, S. Frasier, J. Kurose, F. Junyent, B. Philips, S. Cruz-Pol, and J. Colom, 2005: Distributed Collaborative Adaptive Sensing (DCAS) for improved detection, understanding, and predicting of atmospheric hazards. Preprints, *9<sup>th</sup> Symp. on Integrated Observation and Assimilation System for the Atmosphere, Oceans, and Land Surface*, San Diego, CA, Amer. Meteor. Soc.
- McLaughlin, D.J., E.A. Knapp, Y. Yang, and V. Chandrasekar, 2007: Distributed weather radar using X-Band active arrays. Preprints, *IEEE Radar Conference*, Boston, MA.
- Moisseev, D.N., and Chandrasekar, 2008: Polarimetric spectral filter for adaptive clutter and noise suppression. *Journal of Atmospheric and Oceanic Technology*, early online release, posted January 2008.
- Moisseev, D.N., C.M. Nguyen and V. Chandrasekar, 2008: Clutter Suppression for Staggered PRT Waveforms. *Journal of Atmospheric and Oceanic Technology*, **25**, 2209–2218.
- Nguyen, C.M., D.N. Moisseev and V. Chandrasekar, 2008: A Parametric Time Domain Method for Spectral Moment Estimation and Clutter Mitigation for Weather Radars. *Journal of Atmospheric and Oceanic Technology*, **25**, 83–92.
- NRC (National Research Council), 1995: *Assessment of NEXRAD Coverage and Associated Weather Services*. National Academy Press, Washington D.C.

- NRC (National Research Council), 2002: *Weather Technology Beyond NEXRAD*. National Academy Press, Washington D.C.
- NRC (National Research Council) 2004: *Where the Weather Meets the Road*. National Academy Press, Washington D.C.
- NRC (National Research Council), 2008: *Evaluation of the Multifunction Phased Array Radar Planning Process*. National Academy Press, Washington, D.C.
- NRC (National Research Council), 2009: *Observing Weather and Climate from the Ground Up*. National Academy Press, Washington D.C.
- OFCM (Office of the Federal Coordinator for Meteorological Services and Supporting Research), 2006: *Federal Research and Development Needs and Priorities for Phased Array Radar*. FCM-R25-2006.
- Pepyne, D., D. Westbrook, B. Philips, E. Lyons, M. Zink, and J. Kurose, 2008: Distributed Collaborative Adaptive Sensing networks for remote sensing applications. *Proc. of the American Control Conf.*, Seattle, WA, 4167-4172.
- Philips, B., D. Pepyne, D. Westbrook, E. Bass, J. Brotzge, W. Diaz, K. Kloesel, J. Kurose, D. McLaughlin, H. Rodriguez, and M. Zink, 2007: Integrating End-User Needs into System Design and Operation: The Center for Collaborative Adaptive Sensing of the Atmosphere (CASA). Preprints, *16<sup>th</sup> Conf. on Applied Climatology*, San Antonio, TX, Amer. Meteor. Soc.
- Philips, B., D. Westbrook, D. Pepyne, J. Brotzge, E. Bass, and D. Rude, 2008: User evaluations of adaptive scanning patterns in the CASA Spring Experiment 2007. Preprints, *Proc. of the IEEE 28th International Geoscience and Remote Sensing Symposium (IGARSS)*, Boston, MA.

- Potvin, C.K., A. Shapiro, T.-Y. Yu, J. Gao, and M. Xue, 2008: Using a Low-Order Model to Detect and Characterize Tornadoes in Multiple-Doppler Radar Data. *Monthly Weather Review*, Amer. Met. Soc., in press.
- Proud, J.L., K. Droegemeier, V. Wood, and R. Brown, 2008: Sampling strategies for tornado and mesocyclone detection using dynamically adaptive Doppler radars: A simulated study. *Journal of Atmospheric and Oceanic Technology*, in press.
- Puzella, A. and R. Alm, 2007: Air cooled, active transmit/receive panel array. Preprints, *IEEE Radar Conference*, Lexington, MA.
- Salazar, J. L., R. Medina, E. J. Knapp, and D. J. McLaughlin, 2008: Phase tilt array antenna design for dense distributed radar network for weather sensing. Preprints, *International Geoscience Remote Sensing Symposium*, Boston MA.
- Sarcione, M., N. Koliass, M. Booen, D. McLaughlin, F. Chang, and A. Hajimiri, 2008: Looking ahead: The future of RF technology, military and homeland perspectives. *Microwave Journal*, **51**, 52 - 62.
- Schenkman, A., A. Shapiro, K. Brewster, M. Xue, J. Gao, and N. Snook, 2008: High resolution assimilation of CASA radar data from a tornadic convective system. Preprints, *Symp. Recent Developments in Atmos. Appl. Radar and Lidar*. 20-24 January, 2008, New Orleans, LA.
- Serafin, R. J. and J. W. Wilson, 2000: Operational weather radar in the United States: Progress and opportunity. *Bull. Amer. Meteor. Soc.*, **81**, 809-824.
- Siggia, 1983: Processing phase-coded radar signals with adaptive digital filters. 21<sup>st</sup> *Conference on Radar Meteorology*, Edmonton, Alberta, Canada. 513-518.

- Siggia, A. and J. R. Passarelli, 2004: "Gaussian model adaptive processing (gmap) for improved ground clutter cancellation and moment calculation." *Proc. of the 3<sup>rd</sup> European Conference on Radar in Meteorology and Hydrology*, ERAD, Visby, Gotland, Sweden, 67–73.
- Tabary, P., J. Parent-du-Châtelet, M. Franco, R. Cremonini, C. Ciotti, and G. Vulpiani, 2008: Overview of the weather radar networks and products in the "north-western" Mediterranean region (Spain, France and Italy). Presented at the 2<sup>nd</sup> HyMeX workshop, Palaiseau, France.
- Torres, S. and C. Curtis, 2006: Design considerations for improved tornado detection using super-resolution data on the NEXRAD network. Preprints, *Third European Conf. on Radar Meteorology and Hydrology (ERAD)*, Barcelona, Spain.
- Wang, Y., V. Chandrasekar, and B. Dolan, 2008: Development of scan strategy for dual-Doppler retrieval in a networked radar system. Preprints, *IEEE Intl. Geosciences and Remote Sensing Symposium (IGARSS)*, Boston, MA.
- Westrick, K. J., C. F. Mass, and B. A. Colle, 1999: The limitations of the WSR-88D radar network for quantitative precipitation measurement over the coastal western United States. *Bull. Amer. Meteor. Soc.*, **80**, 2289-2209.
- Willie, D., W. Li, Y. Wang, and V. Chandrasekar, 2006: Attenuation statistics for X-band radar design. Preprints, *Proc. of IGARSS 2006*, Denver, CO.
- Zink, M., E. Lyons, D. Westbrook, V. Chandrasekar, D. Pepyne, B. Philips, and J. Kurose, 2008a: Meteorological Command & Control: Architecture and performance evaluation. Preprints, *Proc. of IGARSS 2008*, Boston, MA.
- Zink, M., E. Lyons, D. Westbrook, J. Kurose, and D. Pepyne, 2008b: Closed-loop architecture for Distributed Collaborative Adaptive Sensing of the Atmosphere: Meteorological Command & Control. *International Journal for Sensor Networks (IJSNET)*, in press.

Table 1. Two-way attenuation (dB) through 10 km of rain.		
Rain Rate (mm/hr)	S-band (10 cm)	X-band (3.2 cm)
4	0.03	1.10
20	0.14	7.79
40	0.27	18.09
100	0.65	55.13

Table 2. Specification comparison between the IP1 (left) and WSR-88D (right) radars.		
Transmitter	Magnetron	Klystron
Frequency	9.41 GHz (X-band)	2.7-3.0 GHz (S-band)
Wavelength	3.2 cm	10 cm
Peak Radiated Power	10 kW	500 kW
Duty Cycle (max)	0.0013	0.002
Average Radiated Power	13 W	1000 W
Antenna Size	1.2 m	8.5 m
Antenna Gain	36.5 dB	45.5 dB
Radome Size	2.6 m	11.9 m
Polarization	Dual linear, simultaneous horizontal/vertical	Single, linear horizontal
Beamwidth	1.8 deg	0.925 deg
PRF	Dual, 1.6 kHz-2.4 kHz	Single, 322-1282 Hz
Pulse width	660 ns	1600-4500 ns
Doppler Range	40 km	230 km
Range Increment	100 m	1000 m*
Azimuth Increment	1 deg	1 deg*
Scan Strategy	60-360 deg adaptive PPI sector scans, 1-30 deg RHI scans	360 PPI scans, 0.5-19.5 deg elevation

\* The NEXRAD “super-resolution” upgrade will reduce the range increment to 250 m and the azimuth increment to 0.5 degrees.

Table 3. Data Products generated by the IP1 radars.

Variable	Units
Reflectivity	dBZ
Velocity	ms <sup>-1</sup>
Spectral Width	ms <sup>-1</sup>
Differential Reflectivity	dB
Differential Phase	Degrees
Cross Pol Correlation	Unitless
Normalized Coherent Power	Unitless
Specific Phase	Radians Per Meter
H Propagation Phase	Radians
V Propagation Phase	Radians

Table 4. IP1 component and O&M costs.

<b>IP1 node component costs</b>	
Antenna	\$8,000
Radome	\$20,000
Tower (6 m)*	\$15,000
Data Acquisition	\$20,000
Transceiver	\$30,000
Elevation Positioner	\$10,000
Azimuth Positioner	\$90,000
Platform, frames	\$10,000
Computers, storage, networking hardware	\$20,000
HVAC	\$6,000
Electricity power-line	\$500
<b>Total</b>	<b>\$229,500</b>
* The 20 m tower at Cyril cost \$120,000; Chickasha uses an existing 20 m tower.	
<b>IP1 yearly O&amp;M costs</b>	
Electric Power	\$2,000
Spare parts/repairs	\$7,500
Networking	\$16,500
Land Lease**	\$0
<b>Total Annual</b>	<b>\$26,000</b>
** Land use is by donation to CASA.	

Table 5. Key specifications for phased-array panels for the dense network application.	
Peak transmit power per panel	10 – 100 W
Panel size	1 m × 1 m
Average beamwidth	2° × 2°
Polarization	dual-linear transmit and receive
Number of panels per site	3 or 4
Azimuth scan range	±45° for a 3 panel installation ±60° for a 4 panel installation
Elevation scan range	0-20° for low level coverage < 3 km 0-56° for coverage up to 21 km

## List of Figures

Figure 1. Dense Network Concept – thousands of small, low-cost, short-range radars mounted on communication-towers, buildings, and other infrastructure elements, communicating with one another to adjust their sensing strategies in direct response to the evolving weather and to changing end-user needs. Provides fine-scale storm mapping throughout the entire troposphere – from the boundary layer up to the tops of storms.

Figure 2. NEXRAD coverage at 3 km above ground level (a) and 1 km above ground level (b). These plots are the center of the beam at 0.5 degrees elevation (NEXRAD lowest allowed tilt, by policy). Coverage data courtesy I. Graffman, NOAA/NWS/OST.

Figure 3. Percent coverage (solid lines) and number of radars needed for CONUS coverage (dashed line) vs. radar spacing. The vertical bar at 345 km is the representative spacing of the NEXRAD radars to the west of the Rocky Mountains, and the vertical bar at 230 km is the average spacing of the NEXRAD radars to the east of the Rocky Mountains. The vertical bar at 30 km is CASA's solution.

Figure 4. Beam height above ground level for a small (1-m antenna) short-wavelength (X-band) radar. The shaded region is the coverage by the 1.8-degree beam at 0.9 degrees elevation angle. The dotted line is the center of the beam. At this lowest tilt the entire beam is below 1 km over a 30 km range.

Figure 5. X-band attenuation statistics for Norman, Oklahoma (Willie et al. 2006). Note that the plot only contains data collected when there was rain falling in the coverage domain of the radar. This single radar attenuation statistic was derived from data from KOUN (a dual-pol NEXRAD).

Figure 6. Sensitivity at 30 km as a function of transmit power for low-power radar technology.

The 80% and 90% attenuation curves incorporate the attenuation data from Figure 5 into the radar equation.

Figure 7. Map of the CASA IP1 testbed in southwestern Oklahoma showing the radar sites and 40 km range rings. Also shown are the NEXRAD radars at Frederick (KFDR) in the lower left and Twin Lakes (KTLX) in the upper right. The rings around the NEXRAD radars are at 40 km and 60 km, respectively.

Figure 8. Architecture of an IP1 radar node (from Junyent, 2007, pg. 49). The tower-top rotating assembly contains the radar antenna, transceiver, data acquisition system, and elevation actuator, all mounted on a frame atop the azimuth positioner. On the radome floor, the non-rotating subsystems include a gigabit Ethernet switch, Ethernet controlled power outlet strip, GPS amplifier, and position controller computer. A gigabit Ethernet optic fiber links the tower top with the data processing server on the ground. The site is connected to the Internet through a radio link.

Figure 9. CASA IP1 polarimetric variables: (a) reflectivity,  $Z_h$ , (b) differential reflectivity,  $Z_{dr}$ , (c) differential phase,  $\phi_{dp}$ , and (d) correlation coefficient,  $\rho_{hv}$ . The CASA IP1 radars are simultaneous horizontal and vertical (SHV) dual-polarization Doppler radars.

Figure 10. Flow diagram depicting the major processing steps of the closed-loop Meteorological Command and Control (MCC) software architecture.

Figure 11. Sequence of sector scans performed around a meteorologically significant feature beginning at 200 m AGL (lowest scan). The sector scan on the left shows the feature at 1, 2, 3, 5, 7, 9, and 11 degrees elevation angle.

Figure 12. CASA Test Network Data – “hook echo” observed by CASA’s pre-prototype network at 200 m altitude (top) compared to a more distant WSR-88D NEXRAD radar located to the southwest of the network (bottom). IP1 has update rates 5 times faster and spatial resolution 8 times finer than the current NEXRAD.

Figure 13. 3-D wind velocity retrieval from the IP1 system. Multiple-Doppler computations have been done with the IP1 network down to 200 m AGL (500m MSL).

Figure 14. Artist’s renditions of two potential electronically scanned (e-scan) radar designs as they might appear when mounted on existing infrastructure such as a cellular communications tower (left) or the side of a building (right). The radar on the left is an example of a phase-tilt deployment (electronically scanned in azimuth, mechanically in elevation). The radar on the right is an example of a phase-phase deployment (electronically steered in both azimuth and elevation).

Figure 15. Signal processing examples from the CASA’s IP1 network: (a) comparing CASA’s dual-polarization attenuation correction technique with the KTLX NEXRAD radar, and (b) illustrating CASA’s ground clutter filtering with adaptive spectral processing.

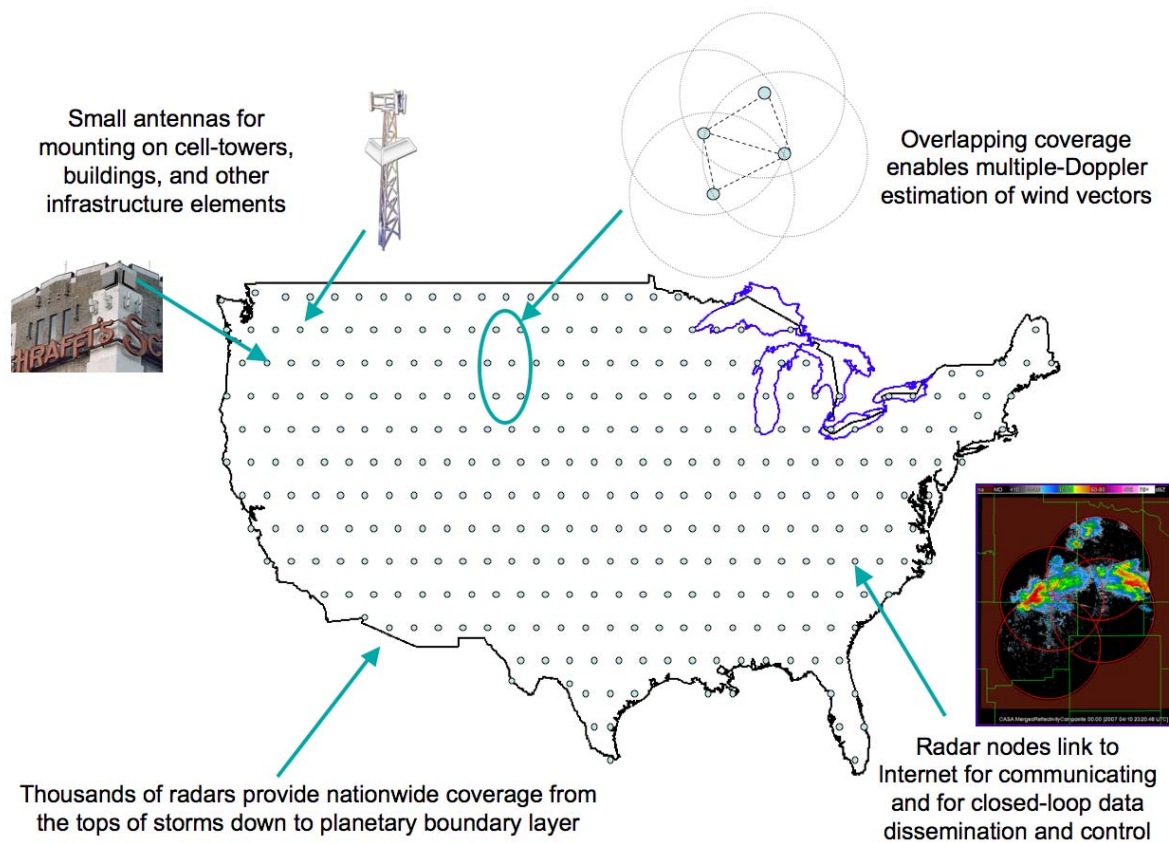
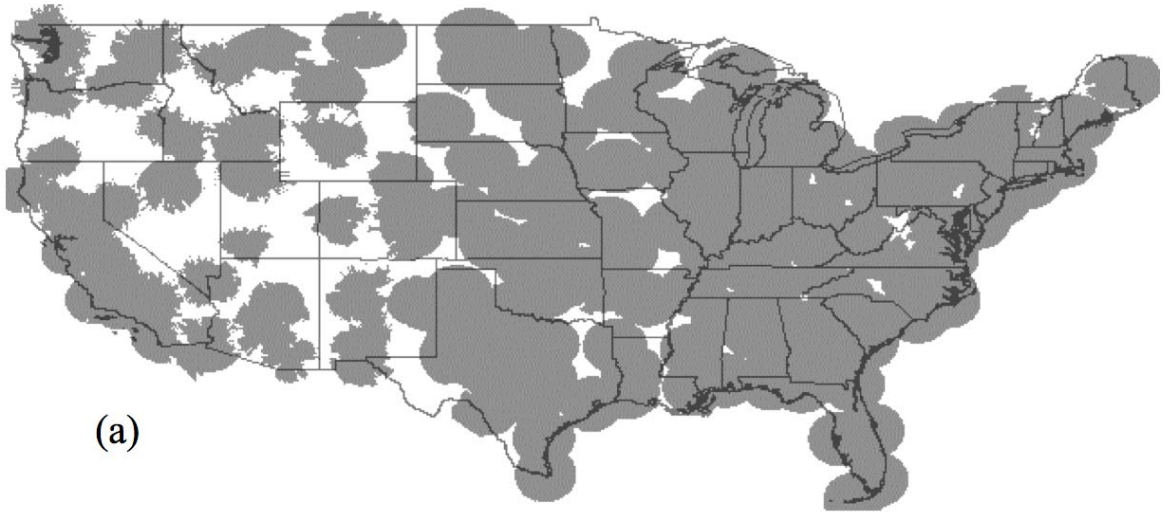
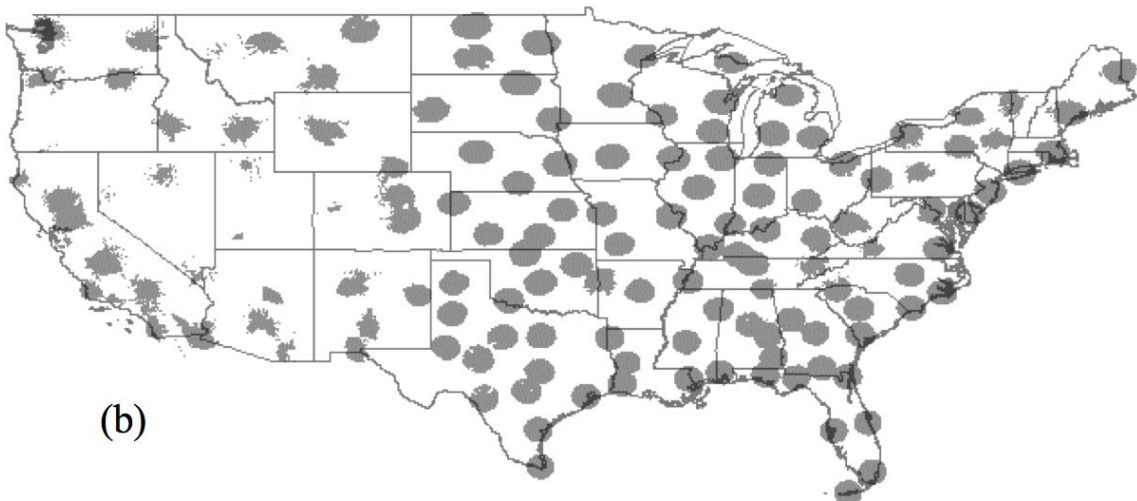


Figure 1. Dense Network Concept – thousands of small, low-cost, short-range radars mounted on communication-towers, buildings, and other infrastructure elements, communicating with one another to adjust their sensing strategies in direct response to the evolving weather and to changing end-user needs. Provides fine-scale storm mapping throughout the entire troposphere – from the boundary layer up to the tops of storms.



(a)



(b)

Figure 2. NEXRAD coverage at 3 km above ground level (a) and 1 km above ground level (b). These plots are the center of the beam at 0.5 degrees elevation (NEXRAD lowest allowed tilt, by policy). Coverage data courtesy I. Graffman, NOAA/NWS/OST.

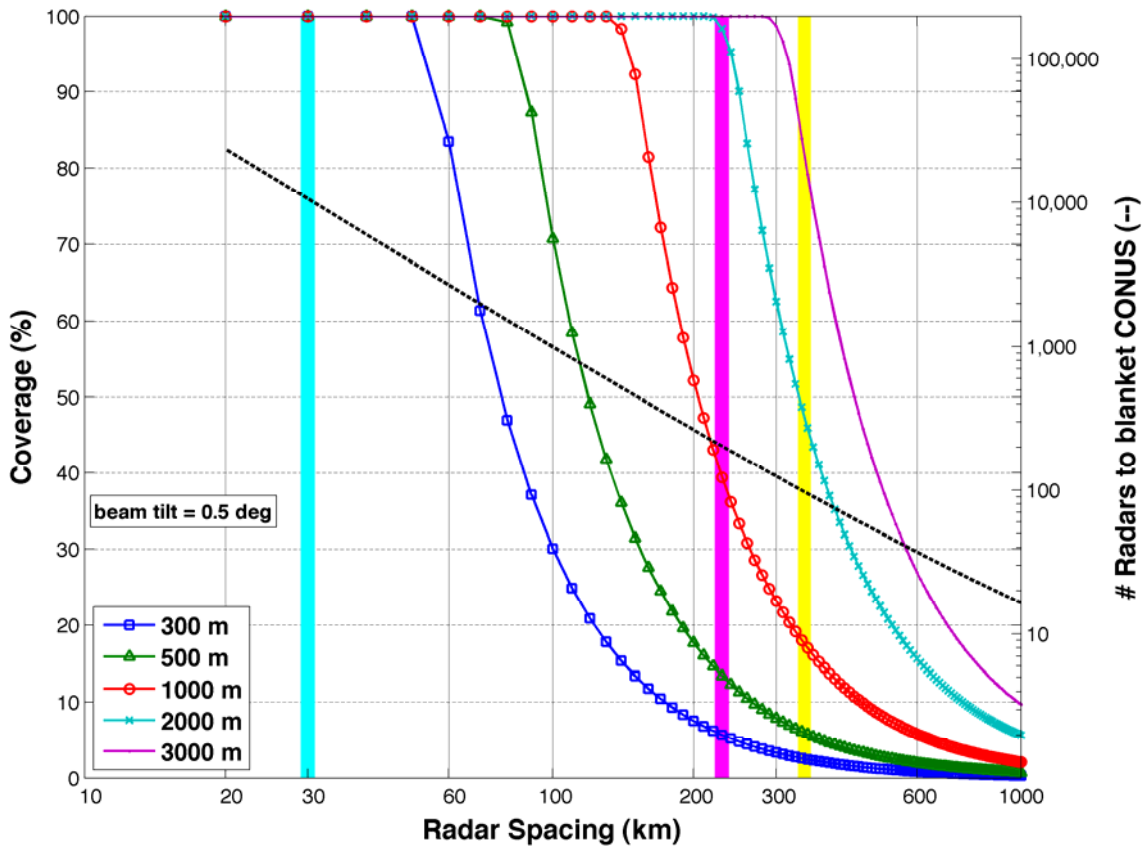


Figure 3. Percent coverage (solid lines) and number of radars needed for CONUS coverage (dashed line) vs. radar spacing. The vertical bar at 345 km is the representative spacing of the NEXRAD radars to the west of the Rocky Mountains, and the vertical bar at 230 km is the average spacing of the NEXRAD radars to the east of the Rocky Mountains. The vertical bar at 30 km is CASA's solution.

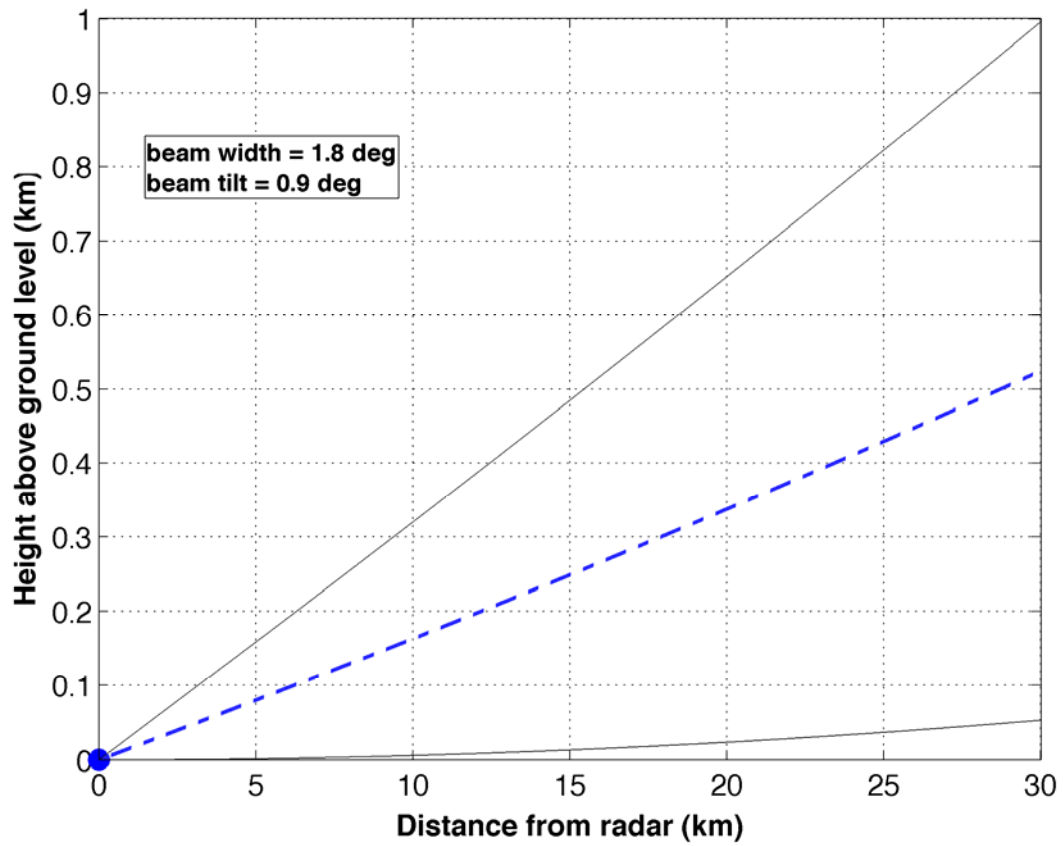


Figure 4. Beam height above ground level for a small (1-m antenna) short-wavelength (X-band) radar. The shaded region is the coverage by the 1.8-degree beam at 0.9 degrees elevation angle. The dotted line is the center of the beam. At this lowest tilt the entire beam is below 1 km over a 30 km range.

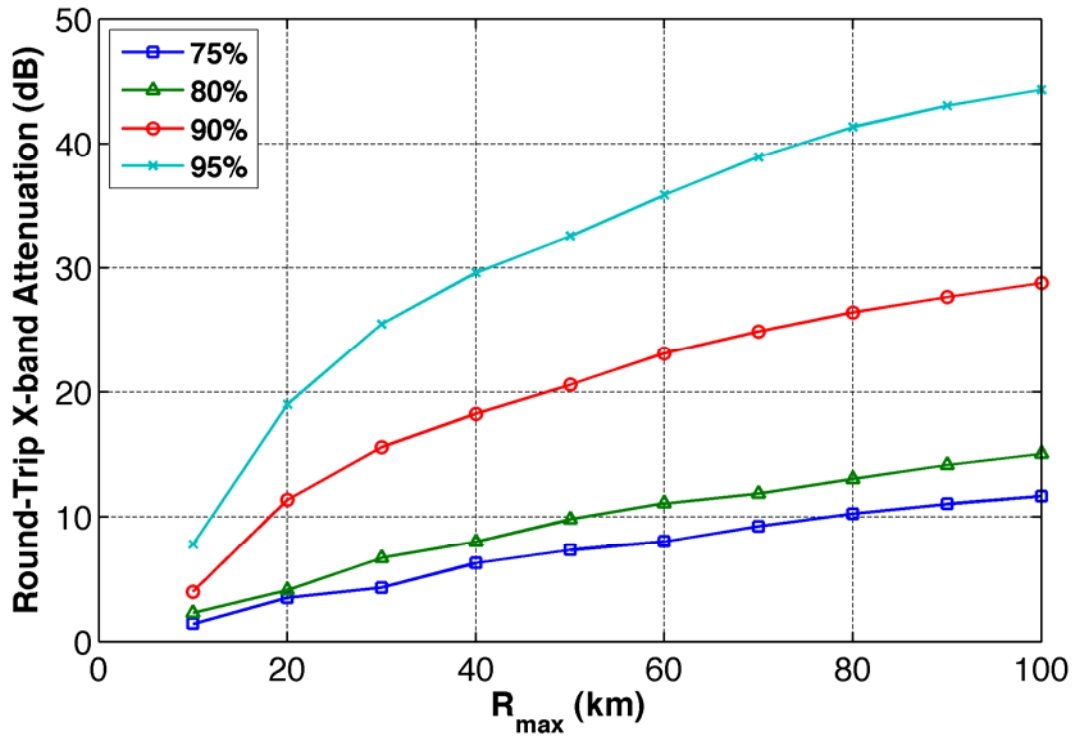


Figure 5. X-band attenuation statistics for Norman, Oklahoma (Willie et al. 2006). Note that the plot only contains data collected when there was rain falling in the coverage domain of the radar. This single radar attenuation statistic was derived from data from KOUN (a dual-pol NEXRAD).

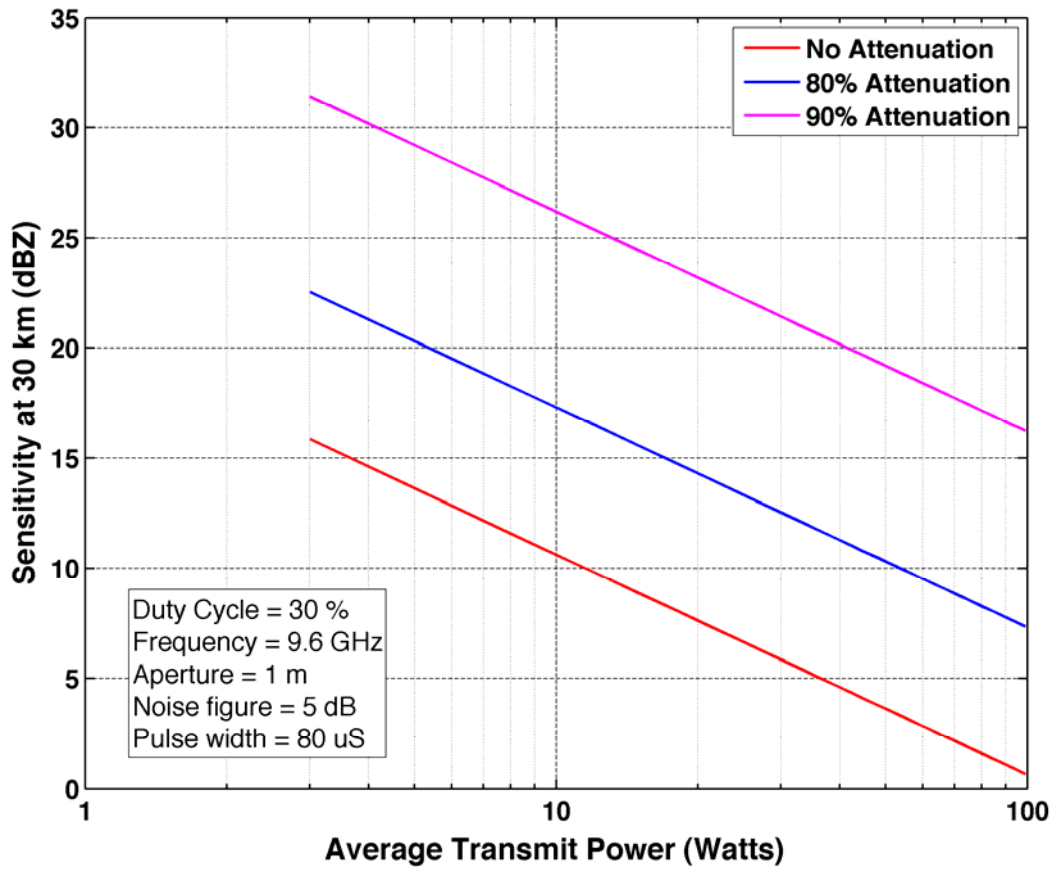


Figure 6. Sensitivity at 30 km as a function of transmit power for low-power radar technology. The 80% and 90% attenuation curves incorporate the attenuation data from Figure 5 into the radar equation.

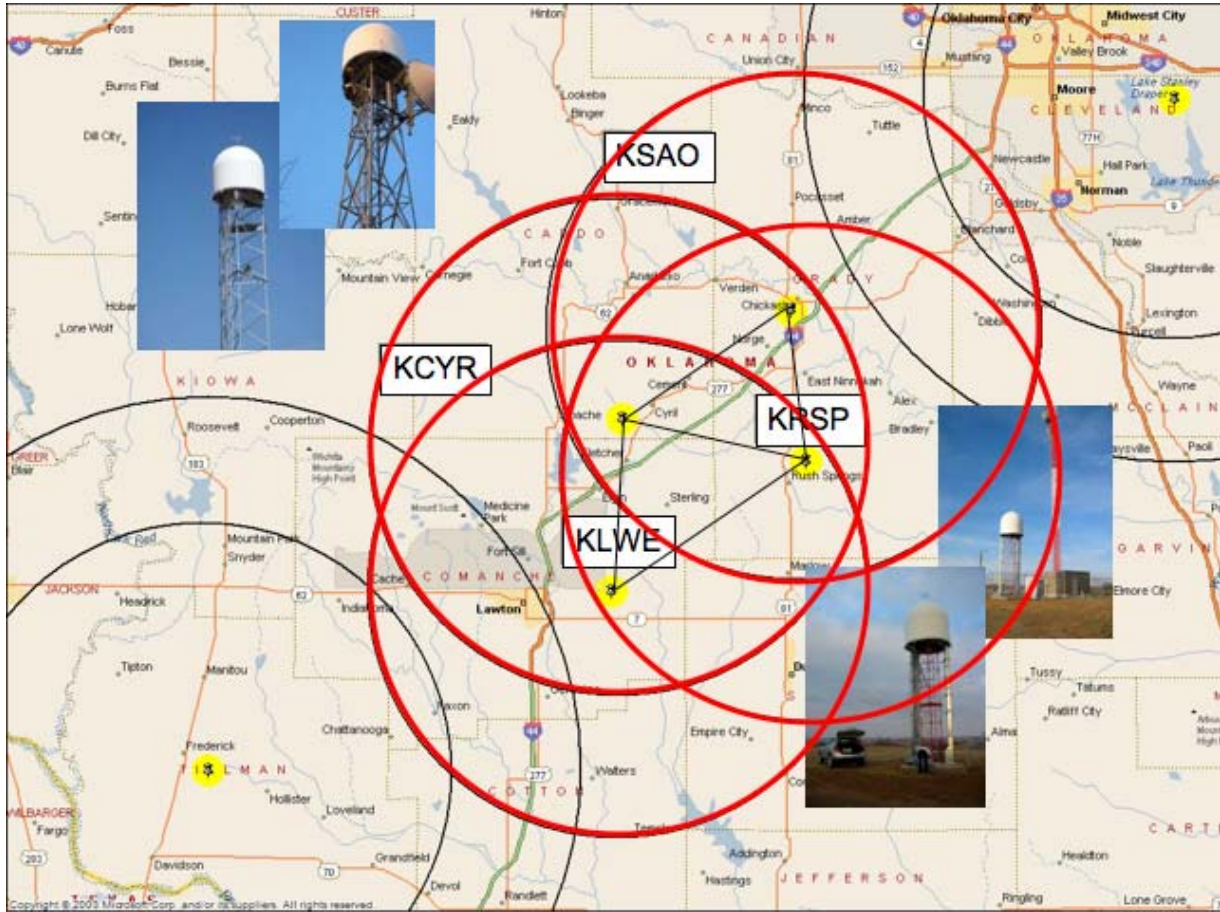


Figure 7. Map of the CASA IP1 testbed in southwestern Oklahoma showing the radar sites and 40 km range rings. Also shown are the NEXRAD radars at Frederick (KFDR) in the lower left and Twin Lakes (KTLX) in the upper right. The rings around the NEXRAD radars are at 40 km and 60 km, respectively.

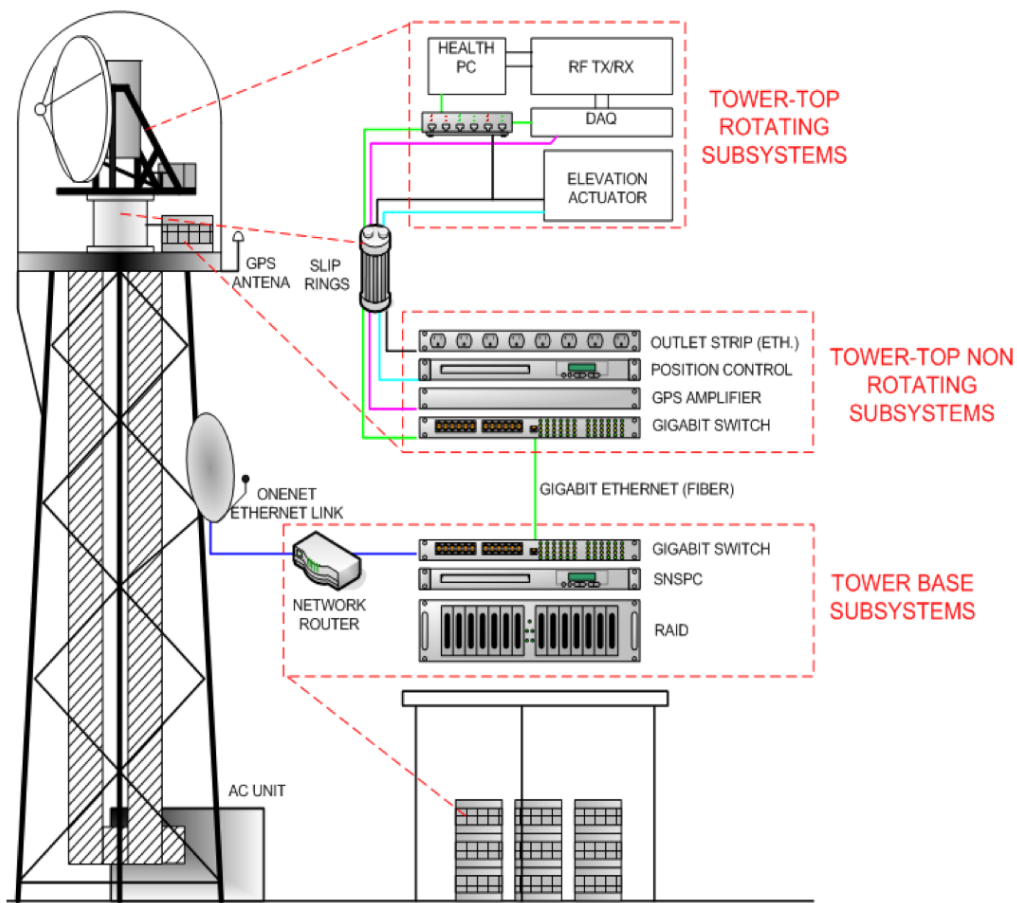


Figure 8. Architecture of an IP1 radar node (from Junyent, 2007, pg. 49). The tower-top rotating assembly contains the radar antenna, transceiver, data acquisition system, and elevation actuator, all mounted on a frame atop the azimuth positioner. On the radome floor, the non-rotating subsystems include a gigabit Ethernet switch, Ethernet controlled power outlet strip, GPS amplifier, and position controller computer. A gigabit Ethernet optic fiber links the tower top with the data processing server on the ground. The site is connected to the Internet through a radio link.

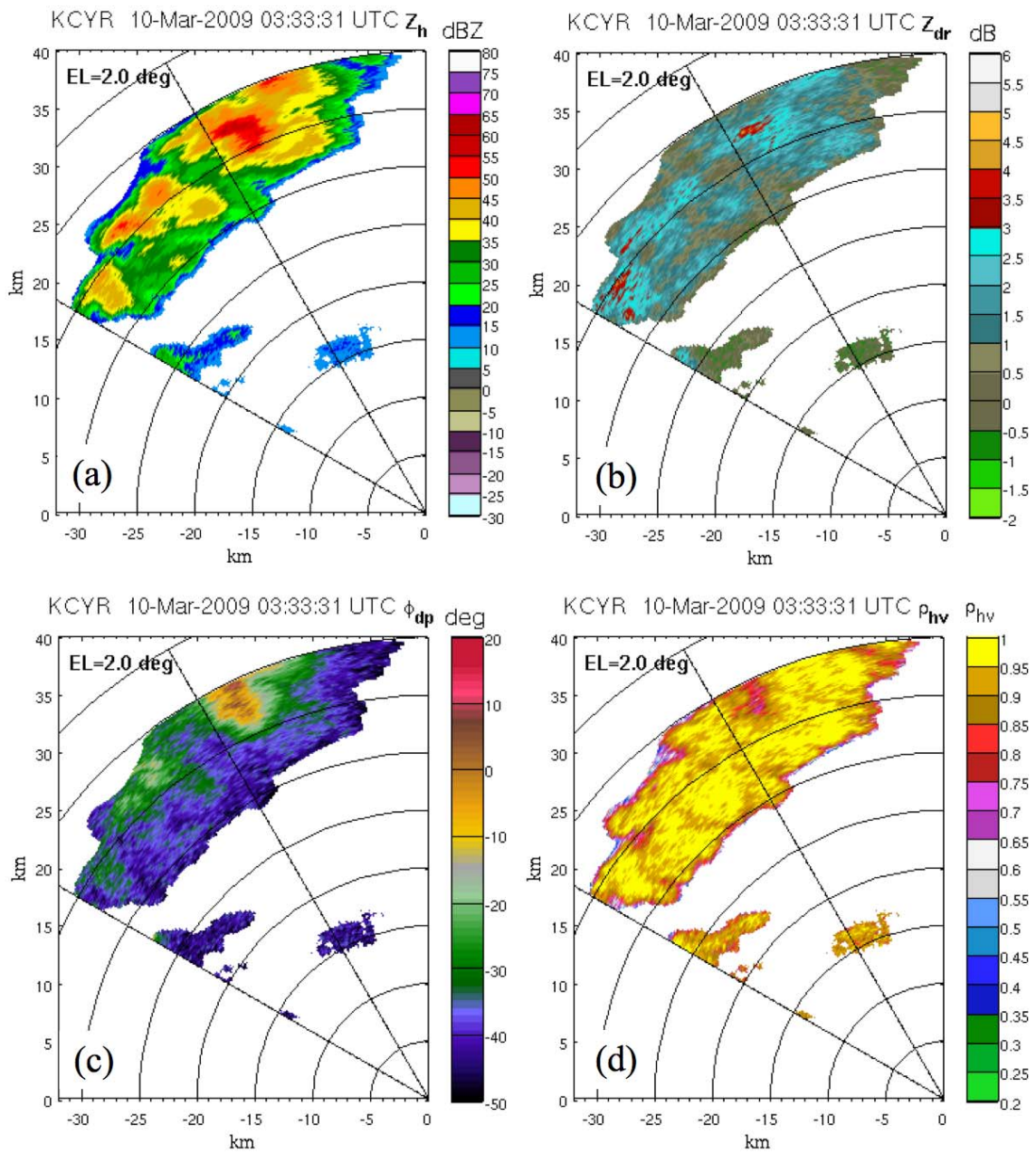


Figure 9. CASA IP1 polarimetric variables: (a) reflectivity,  $Z_h$ , (b) differential reflectivity,  $Z_{dr}$ , (c) differential phase,  $\phi_{dp}$ , and (d) correlation coefficient,  $\rho_{hv}$ . The CASA IP1 radars are simultaneous horizontal and vertical (SHV) dual-polarization Doppler radars.

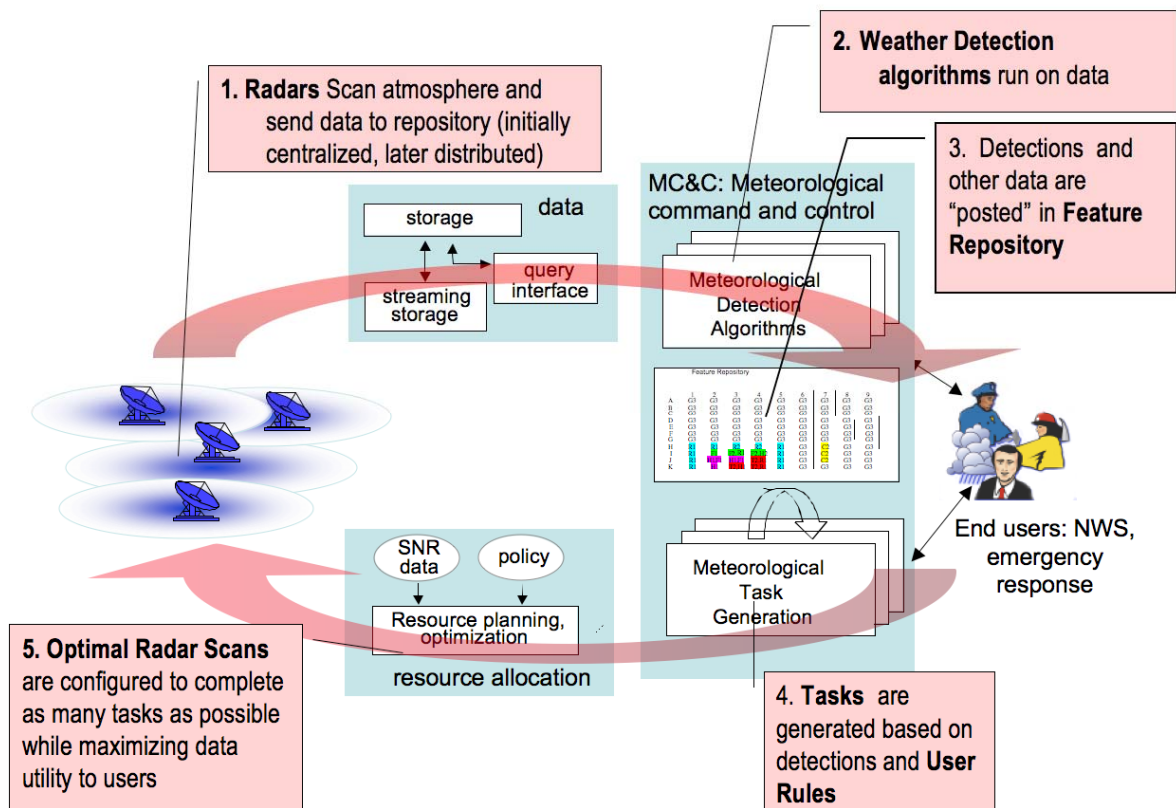


Figure 10. Flow diagram depicting the major processing steps of the closed-loop Meteorological Command and Control (MCC) software architecture.

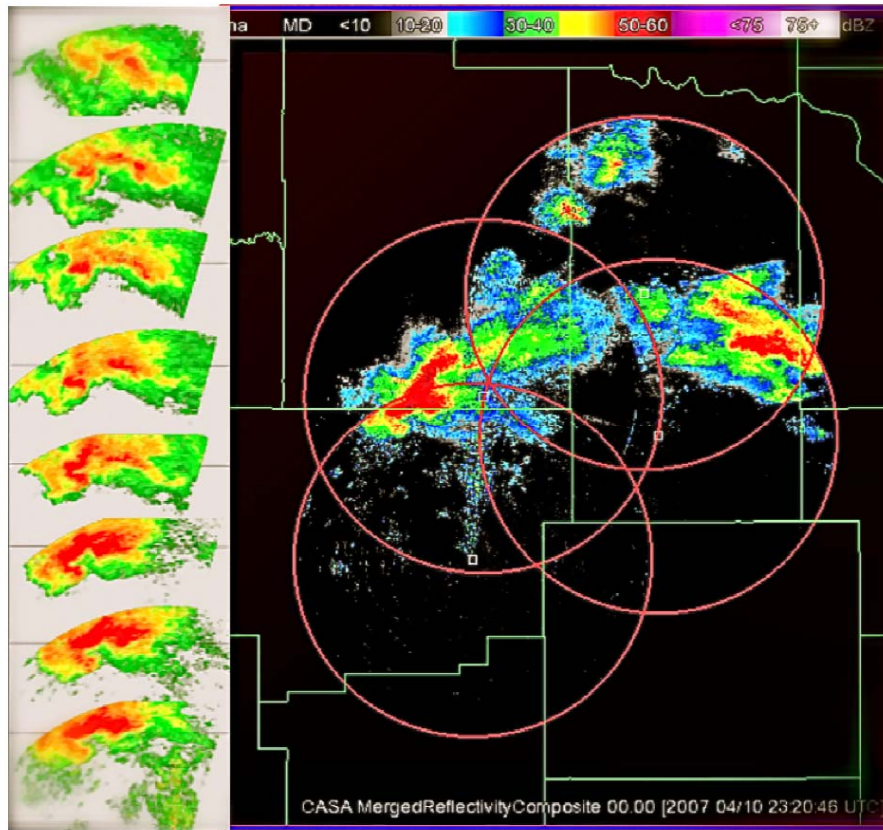


Figure 11. Sequence of sector scans performed around a meteorologically significant feature beginning at 200 m AGL (lowest scan). The sector scan on the left shows the feature at 1, 2, 3, 5, 7, 9, and 11 degrees elevation angle.

May 8-9, 2007

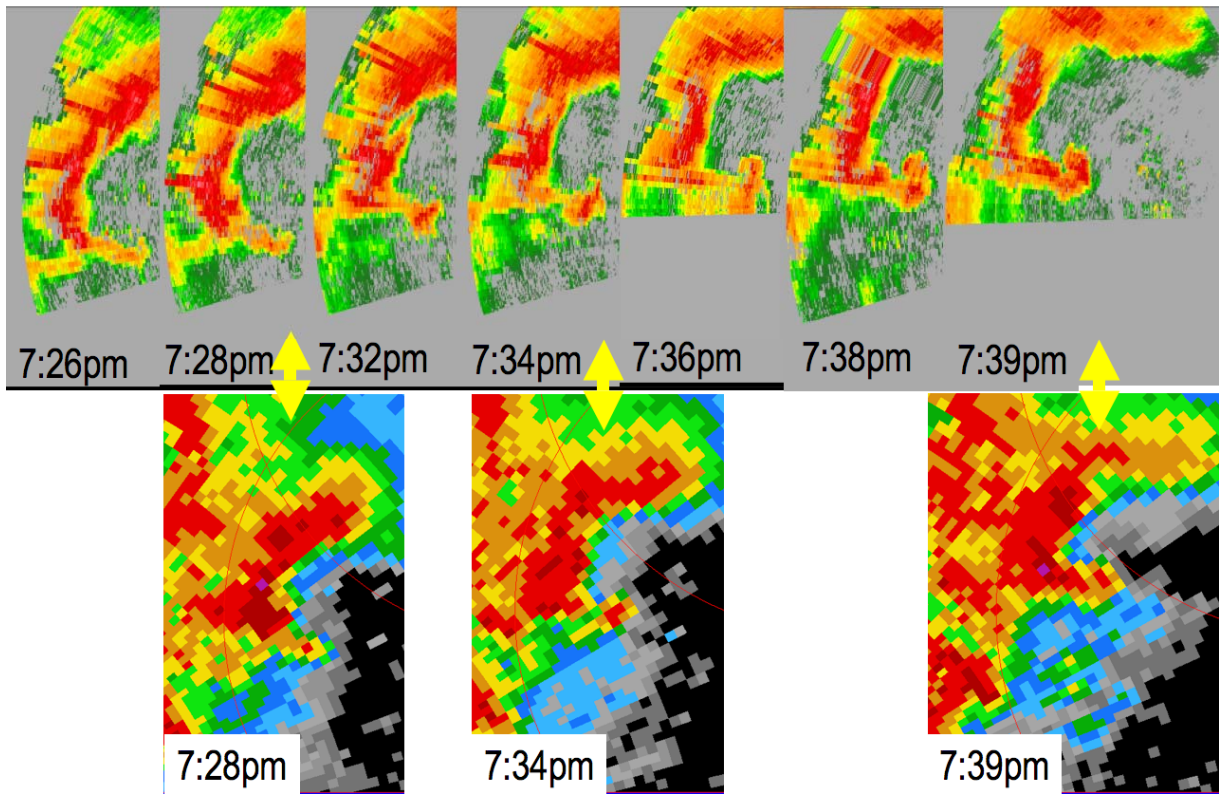


Figure 12. CASA Test Network Data – “hook echo” observed by CASA’s pre-prototype network at 200 m altitude (top) compared to a more distant WSR-88D NEXRAD radar located to the southwest of the network (bottom). IP1 has update rates 5 times faster and spatial resolution 8 times finer than the current NEXRAD.

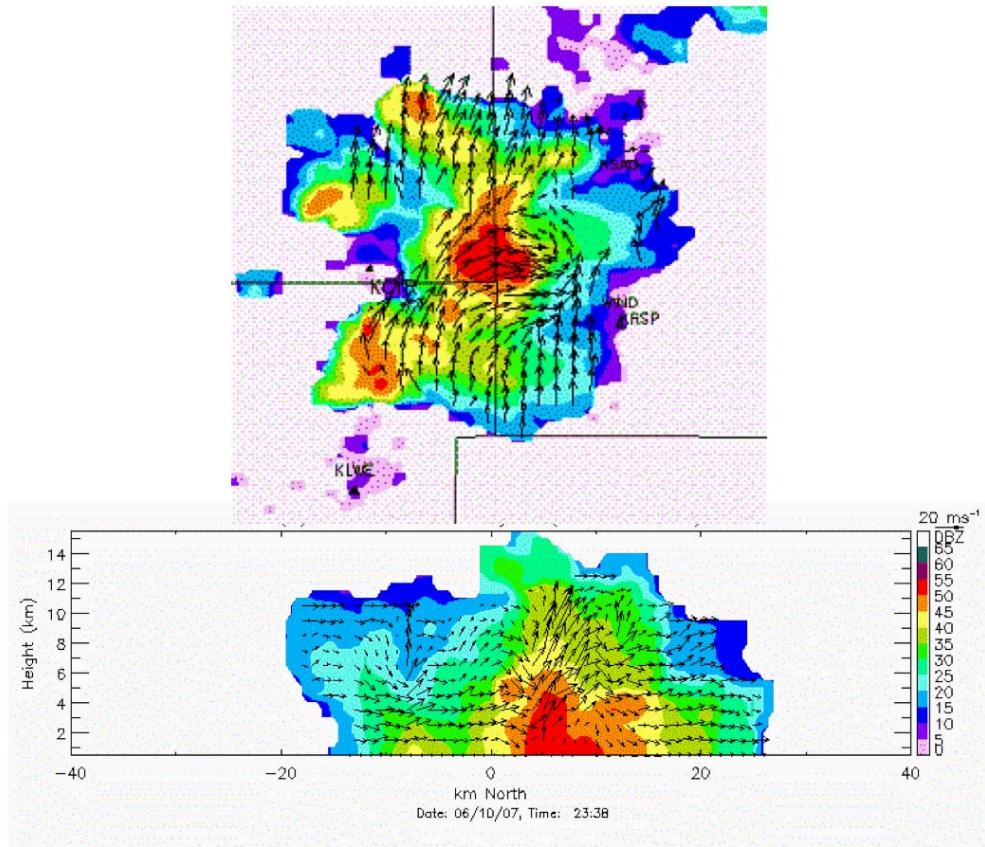


Figure 13. 3-D wind velocity retrieval from the IP1 system. Multiple-Doppler computations have been done with the IP1 network down to 200 m AGL (500m MSL).

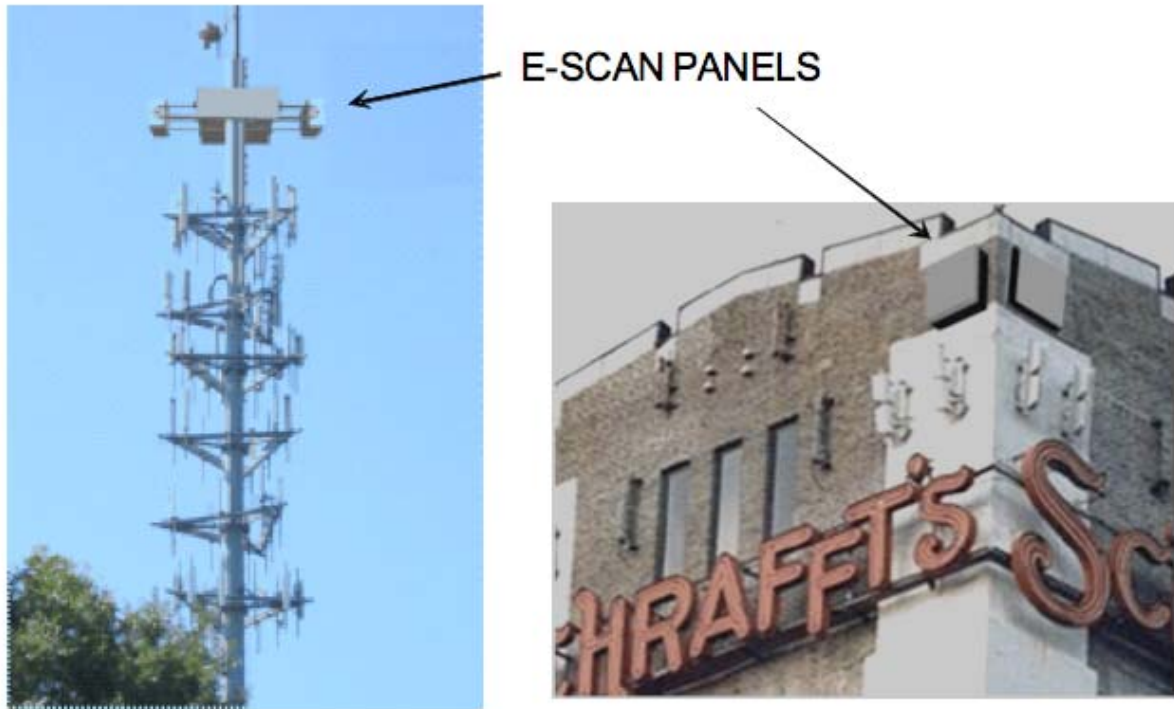
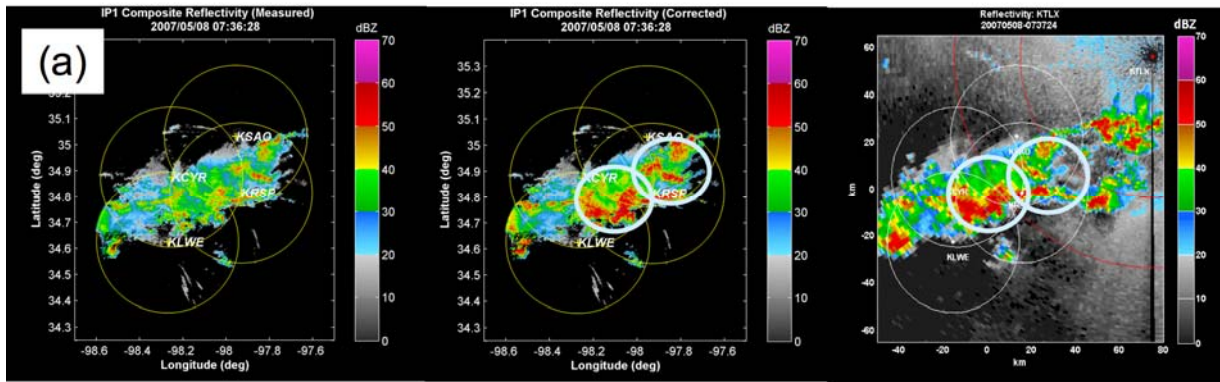


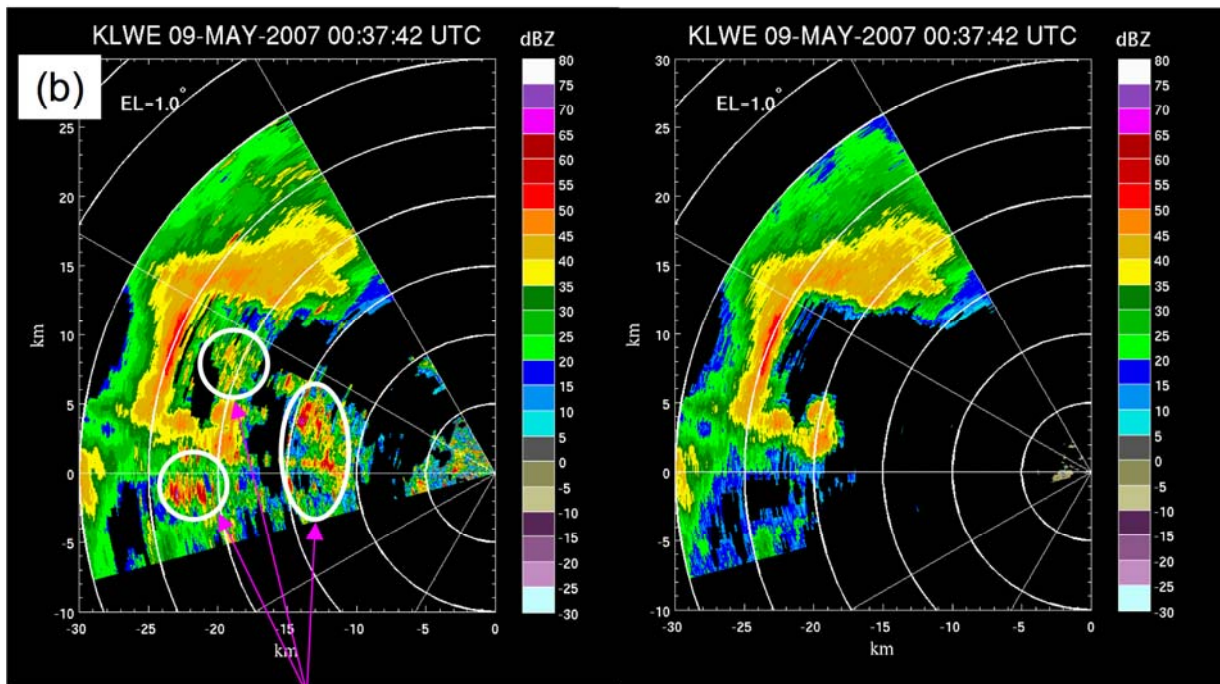
Figure 14. Artist's renditions of two potential electronically scanned (e-scan) radar designs as they might appear when mounted on existing infrastructure such as a cellular communications tower (left) or the side of a building (right). The radar on the left is an example of a phase-tilt deployment (electronically scanned in azimuth, mechanically in elevation). The radar on the right is an example of a phase-phase deployment (electronically steered in both azimuth and elevation).



IP1 measured Z

IP1 corrected Z

KTLX measured Z



Ground clutter

Figure 15. Signal processing examples from the CASA's IP1 network: (a) comparing CASA's dual-polarization attenuation correction technique with the KTLX NEXRAD radar, and (b) illustrating CASA's ground clutter filtering with adaptive spectral processing.